

Article

Tracing and Determining the Duration of Illegal Sand Mining in Specific River Channels in the Limpopo Province

Maropene Tebello Dinah Rapholo ^{1,2,*}, Isaac Tebogo Rampedi ¹  and Fhatuwani Sengani ^{2,*} 

¹ Department of Geography, Environmental Management and Energy Studies, Auckland Park Kingsway Campus, University of Johannesburg, Auckland Park, Johannesburg 2006, South Africa; isaacr@uj.ac.za

² Department of Geology and Mining, Physical and Mineral Sciences, University of Limpopo, Private Bag X1106, Sovenga 0727, South Africa

* Correspondence: maropene.rapholo@ul.ac.za (M.T.D.R.); fhatugeorge@gmail.com or fhatuwani.sengani@ul.co.za (F.S.)

Abstract: Artisanal and Small-scale river sand mining is one of the upcoming activities associated with the environmental crisis concerning the water ecosystem. However, the determination of the duration in which illegal sand mining has occurred, and the future prediction on the extent of river sand mining is not well-established in most of the world. This study aimed to assess the extent of river sand mining activities across some of the catchments in Limpopo province, South Africa and understand the sustainable extraction of sand resources. This was followed by the determination of when sand mining activities commenced in each of the individual catchments. Thus, remote sensing was applied to predict the extent of river sand mining from the year 1992 to 2022, and statistical prediction models were utilised to predict the extent of sand mining for the next 10 years. The results of the study suggest that most of the catchments started to experience illegal sand mining activities from the year 1992, though the extraction was relatively low. Equally, a decrease in vegetation coverage across the river system has been evidenced, which also suggests that the extraction of sand and gravel has been elevated from the year 2010. In terms of the prediction model, the Turfloop River system was predicted to experience a large extraction ratio in the coming 10 years, with about 92.415 ha of land expected to be affected. Meanwhile, the Molototsi River system was denoted to be the least affected river system, with a reduced extraction ratio of about 6.57 ha expected in the next 10 years' time.

Keywords: river sand mining; remote sensing; prediction model; artisanal and small-scale mining



Citation: Rapholo, M.T.D.; Rampedi, I.T.; Sengani, F. Tracing and Determining the Duration of Illegal Sand Mining in Specific River Channels in the Limpopo Province. *Sustainability* **2023**, *15*, 13299. <https://doi.org/10.3390/su151813299>

Academic Editors: Peng Hou, Jinbao Jiang, Hao Sun and Yuebin Wang

Received: 10 July 2023

Revised: 8 August 2023

Accepted: 29 August 2023

Published: 5 September 2023



Copyright: © 2023 by the authors. Licensee MDPI, Basel, Switzerland. This article is an open access article distributed under the terms and conditions of the Creative Commons Attribution (CC BY) license (<https://creativecommons.org/licenses/by/4.0/>).

1. Introduction

Sand mining activities, particularly uncontrolled or illegal sand mining activities, threaten the water quality of affected streams and the safety of river-based sporting and associated activities [1]. As a result, both central and local governments in most countries restrict sand mining operations [1]. For example, in China, governments at various levels have formulated laws and regulations to prohibit illegal sand mining. However, despite such measures, illegal sand mining activities are still rampant in regions such as the Yangtze River Basin, the Yellow River Basin, the Pearl River Basin and the Huaihe River Basin [2–5]. These increases in sand extraction are partially driven by incomes derived from such activities [6]. Moreover, illegal sand mining is typically covert, mobile, and a fragmented activity, and therefore, it can be difficult to detect and manage timeously [6].

As a result, illegal river sand mining is becoming a widespread environmental problem in countries like China [7], Bangladesh [8], India [9,10], Kenya [11,12], Nigeria [13,14], South Africa [15–20] and Botswana [21]. Within these countries, such mining activity is driven by different factors. For the most part, it appears that illegal sand mining is necessitated by the need to meet some of the socioeconomic needs of people who practice it.

Illegal sand mining, by the nature of its scale, lends itself under the broad umbrella of Artisanal Small Scale Sand Mining (ASM), a supposedly legal framework whose regulation is problematic to implement for many governments across the globe [22]. In Africa, ASM is the 'brainchild' of the African Mining Vision (AMV), whose aim is to transform the African mining industry into a knowledge-based one and an accommodative industry to absorb several role players who are willing to participate in the mining sector [22]. However, the lack of a consistent framework to both classify and regulate the ASM sector has given rise to unregulated and hazardous mining practices [22]. For the most part, Gathogo and Amimo [23] conceptualised ASM in terms of its simplicity, where one needs only the simplest of tools and largely informal activities without following much protocol. Zvarivadza [24] further refers to ASM as the exploitation of marginal ore deposits using rudimentary tools, such as picks, shovels, wheelbarrows, panning dishes, and so on. Similarly, Rupprecht [25] described ASM as manual, smallest and simplest mining operations that involve the use of simple tools with basic mining and processing techniques and are carried out predominantly in rural areas.

The exploitation of sand deposits by humans is receiving global attention due to the negative environmental impacts associated with it [17]. Sand mining has expanded at an exponential rate globally because sand is a critical natural resource whose utilisation is leading to the construction of many well-known infrastructures like modern skyscrapers across many cities in the world [7]. Similarly, the impacts of exploiting sand deposits by illegal river sand mining have been studied globally [7].

As indicated by previous researchers [20,26], the Limpopo province has been experiencing illegal river sand mining for some time. Two rivers, namely, Nzhelele and Mokolo, which are some of the main river catchments in the province, amongst others, have been investigated. However, these studies were rather confined to very small areas given the size of the Limpopo Province, to the exclusion of other important river systems such as Lephalele, Letaba and Lepelle (Olifants), which have not been systematically investigated. Furthermore, the few previous studies that were conducted [17,20–26] focused rather on a limited time frame regarding their data collection and analyses. Thus revealing only a partial state of affairs regarding the extent of this environmental problem in this province.

Unfortunately, sand mining causes a myriad of negative environmental impacts on susceptible river channels and natural ecosystems. Given the previous discussions, a few questions can be asked at this point. When did illegal river sand mining commence in the various catchments in the Limpopo province? To what spatial extent has river sand mining gone? What are the environmental impacts associated with illegal river sand mining? Answering these questions may generate an understanding of the impact and occurrence of illegal river sand mining across catchments in the Limpopo province. Therefore, the current study seeks to identify and assess when illegal river sand mining commenced in the Limpopo province, along with an explanation of the patterns it is taking in some of the catchments.

2. Materials and Methods

2.1. Description of the Study Area

The study was carried out in Limpopo province, South Africa. The province is located in the northernmost region of the country and shares international boundaries with Botswana, Mozambique and Zimbabwe. The province covers an area of 125,755 km², accounting for 10.4% of the total national area of South Africa, with a population of about 5.4 million, based on StatsSA 2019. There is a wide range of landscapes in this region, from the Bushveld to the scenic mountains covered in indigenous forests and untouched savannah wilderness [27]. The Limpopo is one of the 9 provinces in South Africa with 5 district municipalities (Capricorn, Vhembe, Sekhukhune, Waterberg and Mopani) and 25 local municipalities.

In terms of hydrology, the province falls under the Limpopo River Basin (LRB) and is located between latitudes 20° S and 26° S and longitudes 25° E and 35° E, and some of the

important water catchments are shared with neighbouring countries, such as Botswana, Mozambique, and Zimbabwe. The basin covers an area of approximately 430,000 km² with altitudes ranging between 150 m and 1200 m. Major rivers in the LRB are the Marico, Crocodile, Matlabas, Mokolo, Lephala, Mogalakwena, Sand, Nzhelele, Luvuvhu, Lepelle and Nwanedi rivers. However, other major river systems include Mokolo, Lephala, Mogalakwena, Sand, Luvuvhu, Letaba and Lepelle (Olifants) (Figure 1). Furthermore, more than 80% of the population depends on these corridors to supply water for agricultural, mining, industrial and domestic uses.

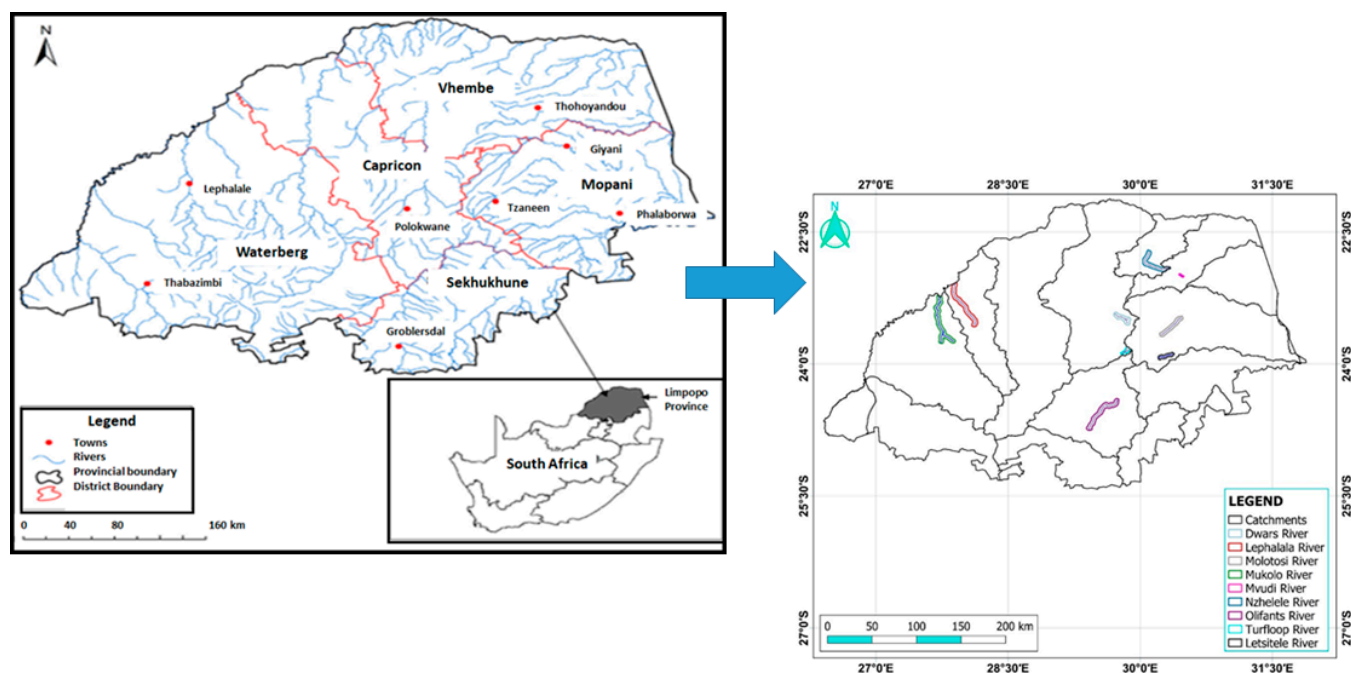


Figure 1. Locality map with river catchments of the Limpopo River Basin in the Limpopo province.

Owing to land use pressures in some of the catchments, the water quality across the abovementioned main rivers has been negatively impacted (Limpopo Basin Permanent Technical Committee (LBPTC 2010)). To mention the few contributing factors, Ashton et al. [28] reported that water resources in most of the sub-catchments in the Limpopo River basin are negatively impacted by mining activities and poorly managed waste disposal facilities. Other point sources of pollutants include traditional and cultural practices whereby local inhabitants wash their dirty laundry in river water, thus releasing copious amounts of wastewater downstream. Similarly, nutrient enrichment released from commercial and subsistence agricultural practices adds to the pollution load of affected rivers.

2.2. Methods

Multispectral sensors, such as Landsat, ASTER and Sentinel2, have been utilised to map mining activities by detecting changes in land cover/land use (LULC) and calculating spectral indices, such as normalised difference vegetation index (NDVI). Advantages of these sensors include their ability to provide cyclic observations, which can provide periodic updates of surface mining activities, cost-effectiveness, extensive areal coverage and medium spatial resolution: Sentinel (10 m), ASTER (15 m) and Landsat (30 m). Landsat was launched in 1972, ASTER in 1998 and Sentinel in 2015. Since this study is aimed at exploring mining activities during the past three decades, from 1992 until 2022 (in a period space of about 10-year intervals) in Limpopo Province, these multispectral sensors are suitable for this study considering their launching dates. However, the mapping of ground features using images of these multispectral sensors can be affected by (1) external factors,

such as the presence of clouds, which interfere with the extraction of valuable information about ground features, and (2) sensor characteristics, such as spatial resolution. Spatial resolution can be defined as the size of the area represented by pixels in an image. The higher the spatial resolution, the better the clarity and ability to identify small ground features (e.g., small mining areas). Therefore, in instances where all sensors acquired cloud-free multispectral images of a required period (e.g., 2022), the image from the sensor with relatively high spatial resolution was selected.

Sand mining zones appear as bare land surfaces in LULC classification images (LULC maps) and are represented by typically low NDVI values, which enable mining zones to be detectable using the NDVI spectral index. As a result, in addition to Google Earth technology, LULC and NDVI generated from processing multispectral sensor images were used to map mining activities and their areal extent over 30 years (1992 to 2022). Furthermore, a regression analysis using a data analysis tool from Excel was used to develop a simple predictive model for future occurrence and the extent of sand mining activities across the catchments.

2.3. Datasets

This study used a multisource of remotely sensed images, namely a high spatial resolution Google Earth platform, including three multispectral sensors (MS): Landsat, ASTER and Sentinel 2.

2.3.1. Description of Multispectral Sensor Datasets

Landsat is a system of multispectral sensors, with the first Landsat 1 established in 1972 and the latest Landsat 9 launched in 2021. In this study, multispectral images of Landsat Thematic Mapper™ 5 and Landsat Operational Land Imager (OLI) retrieved from <https://earthexplorer.usgs.gov/> (accessed on 15 May 2021) and <https://glovis.usgs.gov/> (accessed on 15 May 2021) were used. Developed by NASA, Landsat 5 was launched from Vandenberg Air Force Base in California on 1 March 1984 and covers a spectral region of visible (VIS), near-infrared (NIR) and midinfrared (MID) with 6 bands and 1 band belonging to thermal infrared (TIR). The VISMID bands are characterised by a spatial resolution of 30 m, while the TIR band has a spatial resolution of 120 m (Table 1). On the other hand, Landsat 8 OLI was also launched on an AtlasV rocket from Vandenberg Air Force Base, California, on 11 February 2013. The OLI measures in the VIS, NIR, and SWIR spectral regions with bands having spatial resolution of 30 m. In addition, OLI provides a panchromatic band, which is characterised by 15 m spatial resolution. Table 1 shows the Landsat bands used in this assessment. These bands were selected based on spatial and spectral resolution, including their ability to map LULC and estimate NDVI values. As stated in by Muavhi [27], the higher the spatial resolution, the better the separability of ground feature types, thus promoting accurate LULC mapping.

ASTER is an advanced multispectral remote imaging instrument launched on board NASA's Terra spacecraft in December 1999. ASTER covers a wide spectral region with 14 bands ranging from the visible to thermal infrared region with high spatial, spectral and radiometric resolution. The resolution varies with spectral region: 15 m in VIS and NIR, 30 m in the SWIR, and 90 m in the TIR spectral region. The ASTER datasets selected for this study are ASTER L1T (Precision Terrain Corrected Registered At Sensor Radiance Product) cloud-free scenes, which were retrieved from (<https://earthexplorer.usgs.gov/>, accessed on 15 May 2021) maintained by the USGS/Earth Resources Observation and Science (EROS) Centre at Sioux Falls, South Dakota. Table 2 shows the ASTER bands used in this assessment. Likewise, these bands were selected based on spatial resolution and spectral resolution, which promote accurate LULC mapping and estimate NDVI values.

Table 1. Characteristics of Landsat imageries used in this study.

Landsat Type	Band ID	Bandwidth (μm)	Spatial Resolution
Landsat 5	Band 1 (Blue)	0.450.52	30 m
	Band 2 (Green)	0.520.60	30 m
	Band 3 (Red)	0.630.69	30 m
	Band 4 (Near infrared)	0.760.90	30 m
	Band 5 (Shortwave Infrared)	1.551.75	30 m
	Band 7 (Shortwave Infrared)	2.082.35	30 m
Landsat 8 OLI	Band 2 (Blue)	0.43045	30 m
	Band 3 (Green)	0.530.59	30 m
	Band 4 (Red)	0.640.67	30 m
	Band 5 (Near Infrared)	0.850.88	30 m
	Band 6 (Shortwave Infrared)	1.571.65	30 m
	Band 7 (Shortwave Infrared)	2.112.29	30 m
	Band 8 (Panchromatic)	0.500.68	15 m

Table 2. Characteristics of ASTER bands used in this study.

Band ID	Bandwidth (μm)	Spatial Resolution (m)
Band 1 (Green)	0.520.60	15
Band 2 (Red)	0.630.69	
Band 3 (NIR)	0.780.86	
Band 4 (SWIR)	1.601.70	30
Band 5 (SWIR)	2.1452.185	
Band 6 (SWIR)	2.1852.225	
Band 7 (SWIR)	2.2352.285	
Band 8 (SWIR)	2.2952.365	
Band 9 (SWIR)	2.3602.430	

Sentinel2 is an earth observation mission from the Copernicus Programme that systematically acquires optical imagery at various spatial resolutions covering VNIR and SWIR with 13 bands (see Table 3). The VNIR and SWIR bands, specifically bands 2, 3, 4, 5, 6, 7, 8, 8a, 11 and 12, are characterised by relatively better spatial resolution (10 m and 20 m) and are used in this study for LULC mapping. The Sentinel2 datasets selected for this study are Sentinel2 cloud-free scenes, which were retrieved from (<https://earthexplorer.usgs.gov/>, accessed on 15 May 2021).

Table 3. Characteristics of Sentinel2B bands used in this study.

Band ID	Central Wavelength (μm)	Bandwidth (μm)	Spatial Resolution (m)
Band 2 (Blue)	0.490	0.65	10
Band 3 (Green)	0.560	0.45	10
Band 4 (Red)	0.665	0.30	10
Band 5 (Vegetation red edge)	0.705	0.15	20
Band 6 (Vegetation red edge)	0.740	0.15	20
Band 7 (vegetation red edge)	0.783	0.20	20
Band 8 (NIR)	0.842	0.115	10
Band 8a (Vegetation red edge)	0.865	0.20	20
Band 11 (SWIR)	1.610	0.90	20
Band 12 (SWIR)	2.190	0.180	20

Five scenes of Landsat TM 5 acquired in 1992 (the initial year of the study period) were used for mapping mining activities within and along the eight rivers considered in this study. Meanwhile, 9 ASTER scenes were used for delineating mining activities in 2002. On the other hand, 1 ASTER scene covering the Mvudi River was used to assess sand mining activities along the Mvudi River in 2012, whereas the remaining rivers were assessed with the aid of Landsat OLI images acquired in 2013. The Landsat OLI images of 2013 for other

rivers were chosen due to the lack of ASTER images acquired in 2012. Landsat Oli was launched in 2013. To study the LULC and NDVI characteristics of 2022 (the final year of the study period), 7 scenes of Sentinel are utilised.

2.3.2. Preprocessing of Remotely Sensed Images

All multispectral images were georeferenced to the Universal Transverse Mercator (UTM) zone 35S with World Geodetic System (WGS) 1984 projection in the ArcGIS environment (ArcGIS version 10.8). The georeferenced images were exported in GeoTiff format for further analysis using ENVI Version 5.0 software. Where rivers extended over multiple scenes, mosaicking was used to merge the scenes into one image file (Figure 2).

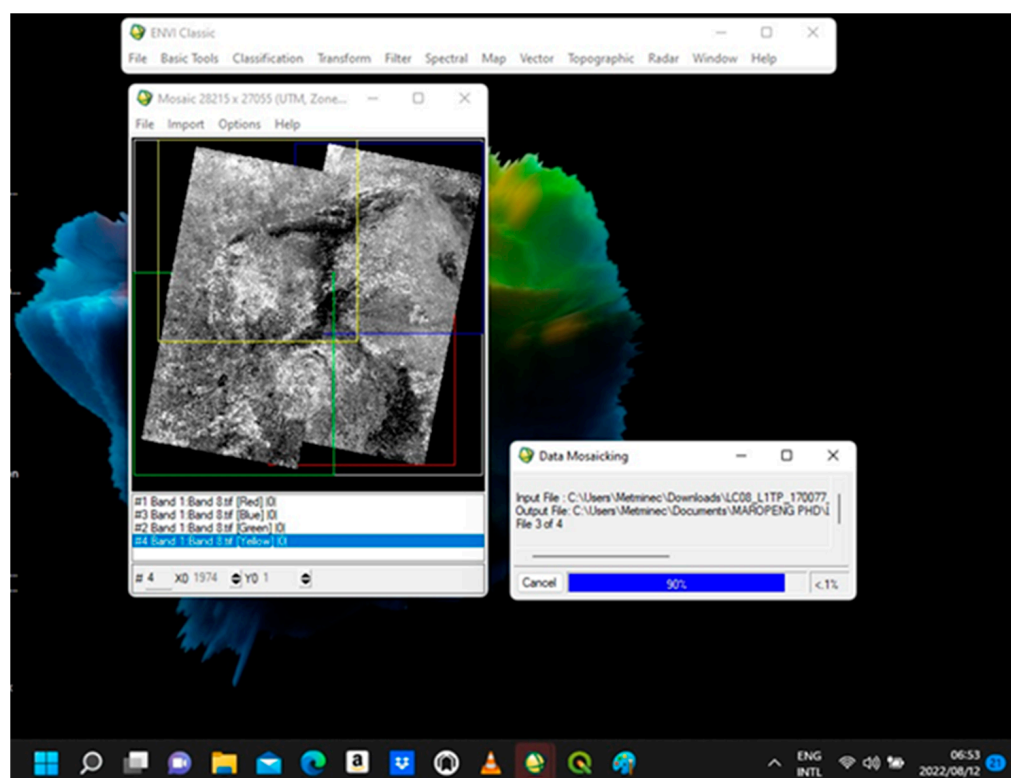


Figure 2. An image showing the process of merging the adjacent scenes.

Multispectral bands for each period (1992, 2002, 2013 and 2022) are layer-stacked to create a multi-band image and then subset to cover the buffered zones of rivers. During the process of layer-stacking of ASTER bands, SWIR bands are resampled to match the spatial resolution (15 m) of VNIR bands for all nine bands to be of the same spatial resolution, which is crucial during image processing. Landsat OLI bands with 30 m spatial resolution are resampled to 15 m spatial resolution based on the panchromatic band. Meanwhile, Sentinel2 SWIR bands were resampled to match the 10 m spatial resolution of VNIR bands. Resampling, also referred to as pan sharpening, aids in attaining better separability of ground feature types from all bands in multiband images.

2.3.3. Atmospheric Correction

The nature of remote sensing requires that solar radiation passes through the atmosphere before it is collected by the sensor. As a result, remotely sensed images include information about both the atmosphere and the earth's surface. To compensate for atmospheric effects and properties, such as the amount of water vapour and distribution of aerosols, atmospheric correction models are used [29]. Various models have been developed to correct atmospheric effects [29]. The selection of a model to implement may depend on factors such as software being used, attribute data of multispectral images, etc. In this

study, the atmospheric correction was carried out with the aid of Log Residuals calibration LULC [30].

2.3.4. LULC Classification

In this study, a supervised classification, which is the image classification based on the user-defined training classes, was used to map LULC. Training classes are representative of materials or ground feature types that will appear on the final image output. The classified LULC is normally subjected to a post-classification process, such as an accuracy assessment, to evaluate the reliability and level of confidence related to the classified LULC map [31]. This process is achieved using testing/validation pixels, which are also representative of ground feature types being mapped but do not form part of training classes.

2.3.5. Selection of Training and Testing Classes of LULC

In this study, the false colour composite (FCC) and true colour composite (TCC) images were used to gather the training and testing datasets of the four LULC classes: vegetation, waterbodies, built-up and bare lands considered in this study. FCC is a combination of three-channel images or bands aimed at creating the false colour of ground features in order to obtain a better visual picture and to improve the targeted features. RGB technique is used to display FCC images by assigning three bands or channel images to the three basic colours (red, green and blue). On the other hand, a TCC image is a combination of three bands that represent the three basic colours (red, green and blue) in order to generate a natural colour form of targeted features. The advantage of a TCC image is that the targeted features appear in their true natural form, which simplifies visual interpretability and the selection of training samples [32].

To generate FCC images, the near-infrared band, red band and green band were assigned red, green and blue, respectively, using the RGB technique. This band combination is widely used in LULC mapping owing to its ability to distinguish ground features effectively. Waterbody appears in blue, vegetation in red, bare land in green and built up in cyan to a whitish colour (Figure 3). Meanwhile, TCC images are generated by assigning the red band, green band and blue band their associated colour (red, green and blue) using the RGB technique.

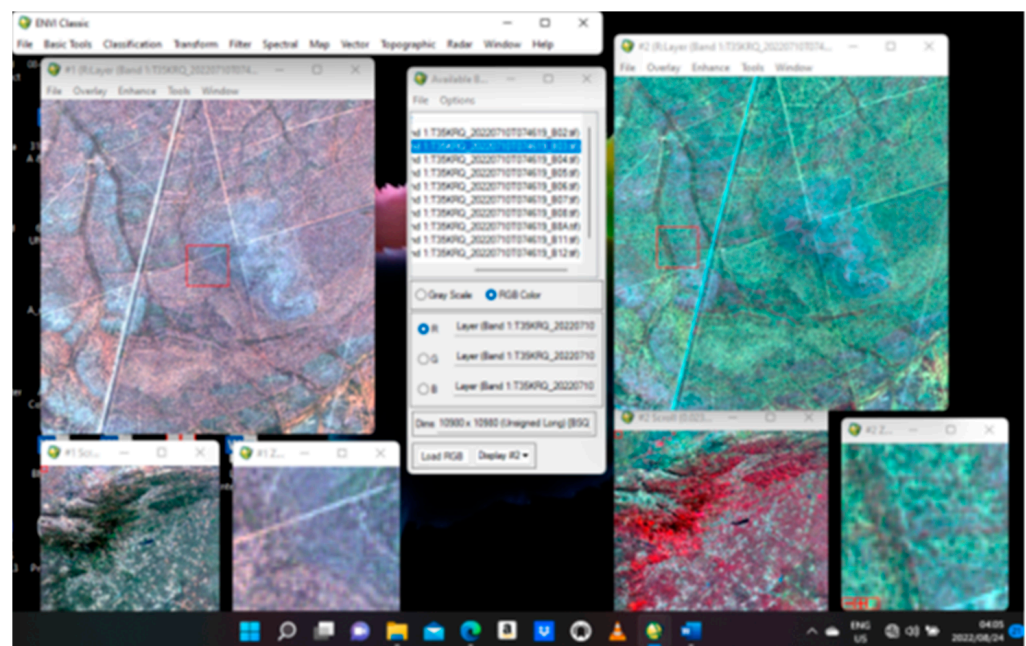
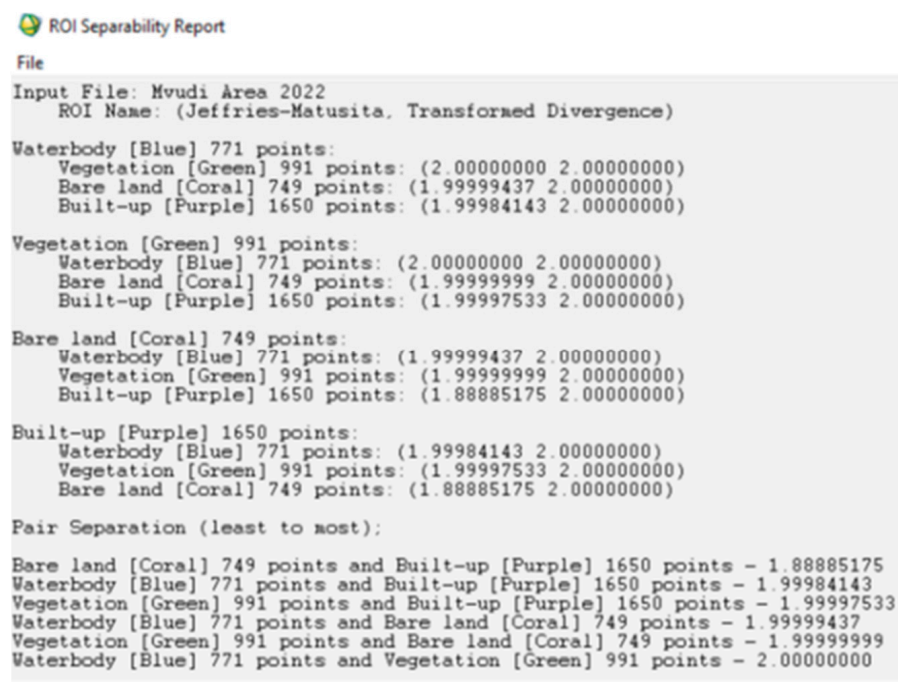


Figure 3. A photograph of TCC image (left) and FCC image (right).

The representative samples of LULC classes were extracted as regions of interest (ROIs), which were then examined for class separability using Transformed Divergence (TD) and Jeffries Matusita Distance (JMD) in the ENVI environment. Separability measures between samples from different LULC classes are necessary to (1) evaluate the quality of the class representative samples, (2) determine the classes with ambiguous boundaries in feature space, where poor classification accuracy is expected, and (3) determine those features where the separability between classes is limited [33,34].

TD and JMD separability measures are an indirect estimate of the likelihood of correct classification between different data sets or derived measures [35]. The TD and JMD separability measures of ROIs/class pairs are reported as values ranging from 0 and indicate how well the classes separate. A value of 0 indicates complete overlap between the signatures of two classes, and 2 indicates a complete separation between the two classes [36], while ≥ 1.5 indicates acceptable separability between classes [37]. In general, values greater than 1.9 between the two classes indicate excellent separability [36]. The LULC classes in this study achieved TD separability measures >1.5 (Figure 4), which can be considered a cutoff point of acceptable separability measures [37]. Built up against bare land attained relatively low separability measures. This can be attributed to spectral similarities between certain roofing and building materials and bare soils. The difficulty in separating these two LULC classes has been demonstrated in the study of Muavhi [31], which was conducted in the Limpopo Province. Nonetheless, all separability measures attained fall above the cutoff point of acceptable separability measures (>1.5) [38].



ROI Separability Report

File

Input File: Mvudi Area 2022
ROI Name: (Jeffries-Matusita, Transformed Divergence)

Waterbody [Blue] 771 points:
Vegetation [Green] 991 points: (2.00000000 2.00000000)
Bare land [Coral] 749 points: (1.99999437 2.00000000)
Built-up [Purple] 1650 points: (1.99984143 2.00000000)

Vegetation [Green] 991 points:
Waterbody [Blue] 771 points: (2.00000000 2.00000000)
Bare land [Coral] 749 points: (1.99999999 2.00000000)
Built-up [Purple] 1650 points: (1.99997533 2.00000000)

Bare land [Coral] 749 points:
Waterbody [Blue] 771 points: (1.99999437 2.00000000)
Vegetation [Green] 991 points: (1.99999999 2.00000000)
Built-up [Purple] 1650 points: (1.88885175 2.00000000)

Built-up [Purple] 1650 points:
Waterbody [Blue] 771 points: (1.99984143 2.00000000)
Vegetation [Green] 991 points: (1.99997533 2.00000000)
Bare land [Coral] 749 points: (1.88885175 2.00000000)

Pair Separation (least to most):

Bare land [Coral] 749 points and Built-up [Purple] 1650 points - 1.88885175
Waterbody [Blue] 771 points and Built-up [Purple] 1650 points - 1.99984143
Vegetation [Green] 991 points and Built-up [Purple] 1650 points - 1.99997533
Waterbody [Blue] 771 points and Bare land [Coral] 749 points - 1.99999437
Vegetation [Green] 991 points and Bare land [Coral] 749 points - 1.99999999
Waterbody [Blue] 771 points and Vegetation [Green] 991 points - 2.00000000

Figure 4. Example of separability measure report.

After attaining acceptable separability measures, individual LULC class was exported to nD Visualizer in the ENVI environment, which is an interactive tool that can be utilised to select groups of pixels into classes [29]. Two subclasses from individual classes were randomly created in the nD Visualizer and then exported to be used as training datasets for supervised classification based on support vector machine (SV) and testing datasets for accuracy assessment based on confusion matrix. Figure 5 shows an example of the main LULC class and its two subclasses representing the training dataset and testing dataset.

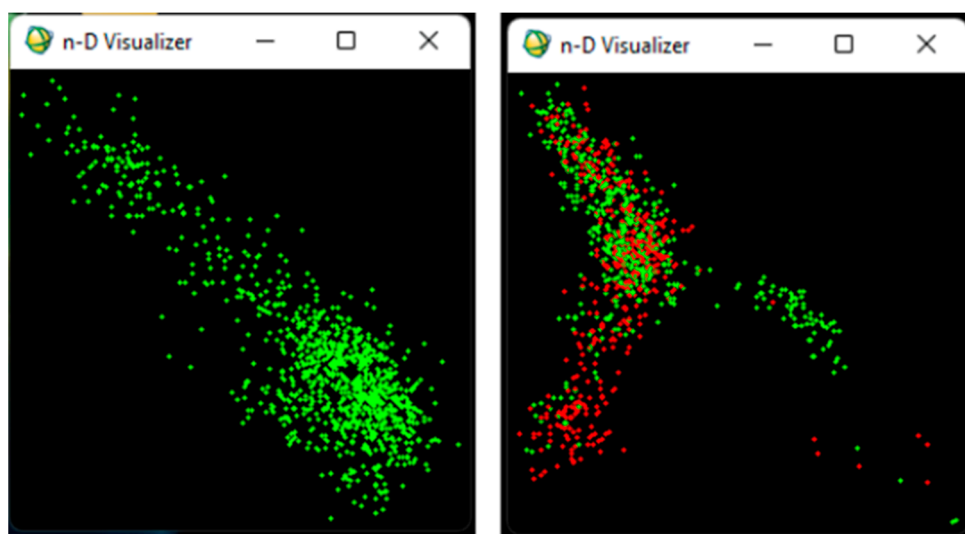


Figure 5. nD visualiser images showing a vegetation main class on the left and two created vegetation subclasses on the right: training (green) and testing (red) dataset.

2.3.6. Support Vector Machine

In this study, the main kernel function, radial basis function (RBFK), was utilised to conduct SVM classification. The mathematical expression of the RBFK is given below [39]:

$$RBFK(x_i x_j) = \exp\left(-g\|x_i - x_j\|^2\right), g > 0 \quad (1)$$

where x_i and x_j are the input vectors, and g is the gamma parameter.

Two key parameters for the RBFK, penalty (C) and gamma, needed to be preselected to generate an optimal SVM model. Parameter ‘ g ’ controls the degree of nonlinearity of the model, whereas parameter ‘ C ’ controls the overfitting of the model by specifying tolerance for misclassification [39]. In this study, the RBFK, characterised by a default gamma value of 0.33 and penalty parameter of 100.00, was used to generate LULC classification maps for the study period. These values have proven to produce accurate LULC mapping in previous studies (e.g., Muavhi [31]).

2.3.7. Accuracy Assessment

In this study, the randomly generated testing subclasses of the main LULC classes were used to assess the accuracy assessment of SVM-generated LULC maps of the study period using a confusion matrix.

In simple terms, the confusion matrix agrees on the testing/validation dataset and interpreted LULC types in the classification map [7,17]. Similarly, with other studies [40], the common accuracy measures used in this study include the overall accuracy and Kappa coefficient (K). Additionally, the accuracy of individual LULC was calculated using the user’s and producer’s accuracy, including commission and omission errors. On the other hand, omission error is the number of validation pixels that are not classified for a land cover type while, in reality, they belong to that LULC type; meanwhile, commission error calculates the number of validation pixels misclassified as belonging to a LULC type while in the ground they represent other land cover types [40].

2.3.8. Normalized Difference Vegetation Index

NDVI is the most used spectral index in mapping vegetation change over time. Generally, surface disturbance associated with mining activities causes changes in surface vegetation cover, which can be detected by NDVI dynamics [41]. NDVI is applied using Near-Infrared (NIR) and red bands. The principle behind the NDVI in vegetation mapping is that the vegetation is highly reflective and absorptive in NIR and visible red, respectively.

The difference between these bands can be used to indicate the presence or absence of vegetation [32,34,42]. Thus, this makes the NDVI a good indicator in reflecting seasonally or periodically dynamic changes in vegetation conditions that may have been triggered by mining activities. The NDVI values range from -1 to 1 , and the common range for vegetation is 0.2 to 1 [40], whereas bare land is typically represented by values < 0 [42]. Therefore, the areas where mining activities damaged vegetation were indicated by low NDVI values (< 0), while the areas where reclamation and restoration have been carried out would be characterised by high NDVI values (> 0). ENVI is used to estimate NDVI values using the following equation:

$$NDVI = \frac{NIR - Red}{NIR + Red} \quad (2)$$

3. Results and Discussions

3.1. Detection of Mining Activities in Different River Channels

3.1.1. Illegal Sand Mining in the Mvudi River System

A total of 23 illegal mining locations were identified along the Mvudi River system. The mining activities were limited to the lower and middle stream sections (Figure 6a) of this channel. The upper stream section is used mainly for agricultural activities. By monitoring the periodic changes of the surface area along the Mvudi River using Google Earth technology, it was found that mining activities predominated the second half of the last decade (2012–2022). Among the affected sites, one location was mined from the year 2002 until the year 2012, and the mining activities of the remaining 22 locations happened after the year 2012 (Figure 6b). With regard to the areal extent of mining activities under consideration, in the year 2002, the extent of such activities in one of the locations covered an area of 1.7 ha. Subsequently, they increased to 1.8 ha in the year 2012. Thereafter, operations ceased. However, later on, 22 new mining sites appeared, and they extended geographically to cover an area of 8.1 ha in the year 2022.

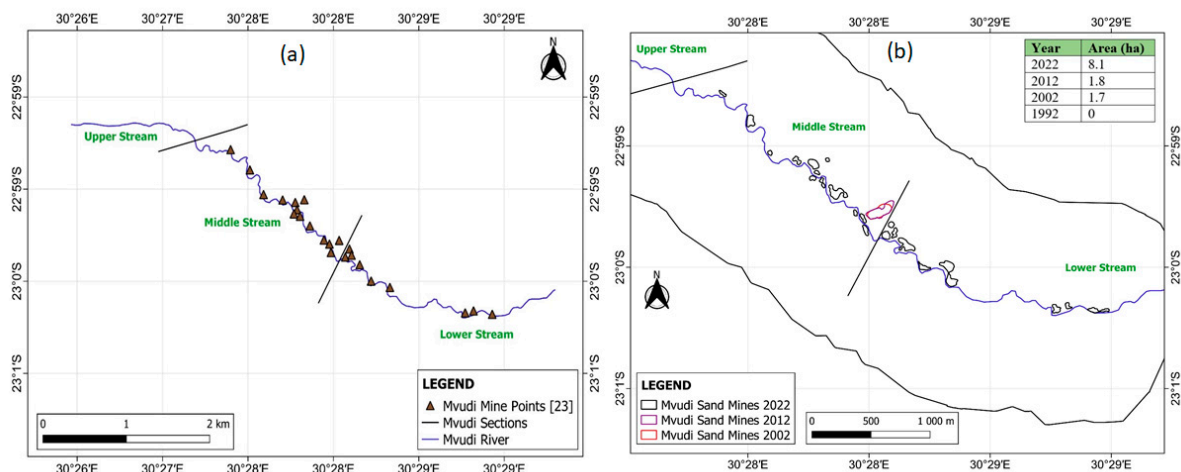


Figure 6. (a) Sand mining points, (b) Areal extent of mining activities over the study period.

The sudden increase in mining activities after the year 2012 coincided with the construction of tarred roads east of the Mvudi River. These roads connect local areas and later join the R525 main road, which is located to the north of this river. Previous research has shown that well-developed access roads may increase the occurrence and spread of artisanal and small-scale mining activities in vulnerable catchments [41].

The LULC maps that were classified and based on the training classes of LULC extracted from TCC and FCC images, and the application of the SVM algorithm are displayed in Figure 7. These maps attained overall accuracies and Kappa coefficients of over 80% and 0.8, respectively (overall accuracies = 99.87% and Kappa coefficients

= 0.99), which represent reliable LULC mapping [43]. In general, natural vegetation and waterbodies achieved better individual accuracies (producer's and user's accuracy), whereas bare land and built-up areas attained relatively low individual accuracies, which can be attributed to their low separability measures resulting in the misclassification of bare land as built-up areas.

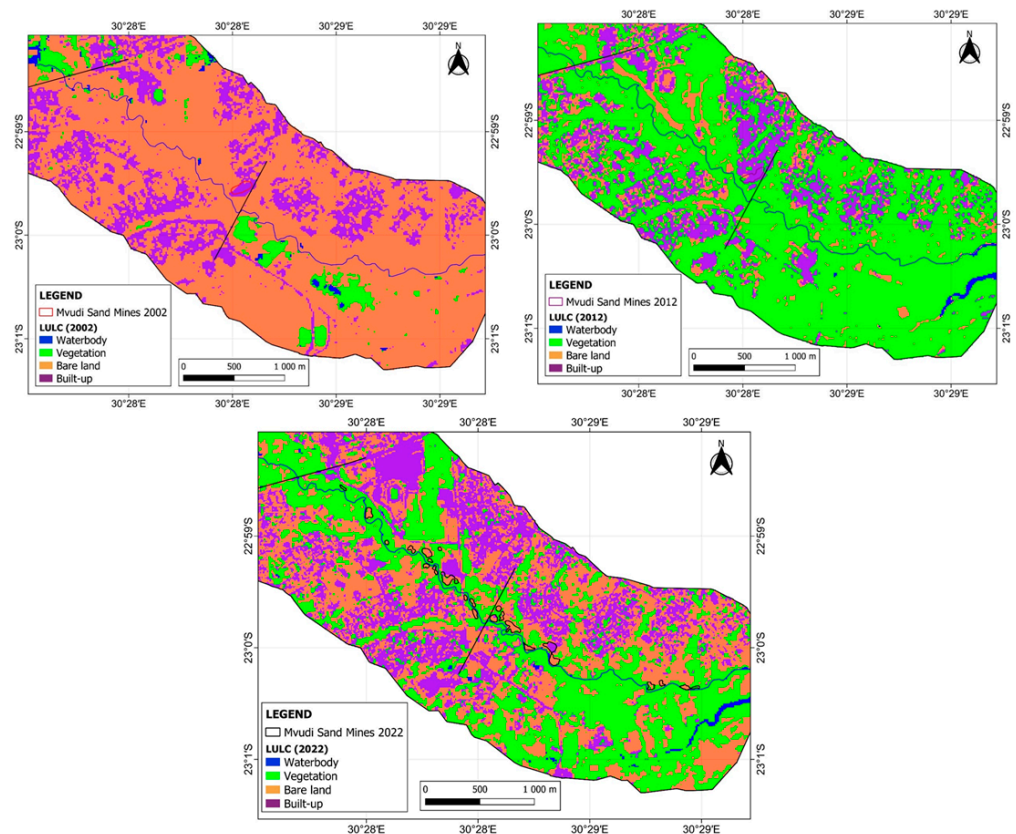


Figure 7. LULC maps of the periods of active mining industries in the Mvudi River.

Some of the building materials used in the surrounding residential areas are sourced from illegal mining activities, and they show some spectral similarities, thus decreasing the separability of the two LULC classes. Nonetheless, most illegal mining locations showed distinctive patterns that set them apart from their surrounding areas. Such patterns are distinctive when polygons of mining locations extracted from Google Earth images are superimposed over LULC maps. Such mining polygons are mostly associated with pixels classified as bare land and, to a lesser extent, as built-up areas due to low separability measures between the two LULC classes.

NDVI maps for periods of active mining activities (2002, 2012 and 2022) were also generated to help in assessing vegetation conditions and to determine the extent to which illegal sand mining activities affected the vegetation along the Mvudi River. The NDVI maps were segmented into five discrete classes for better visual interpretation (Figure 8). The NDVI values for the years of active mining activities were less than 0.2. NDVI values below 0.2 indicate low vegetation productivity or poor vegetation condition and predominance of bare land, which can be associated with mining activities. The rapid decrease in vegetation cover represented by NDVI indicates negative impacts induced by river sand mining along the channel bed. Previous studies [43,44] confirmed that when sand and gravel mining is unregulated and takes place in an uncontrolled manner, the outcome is usually the alteration of natural river equilibrium.

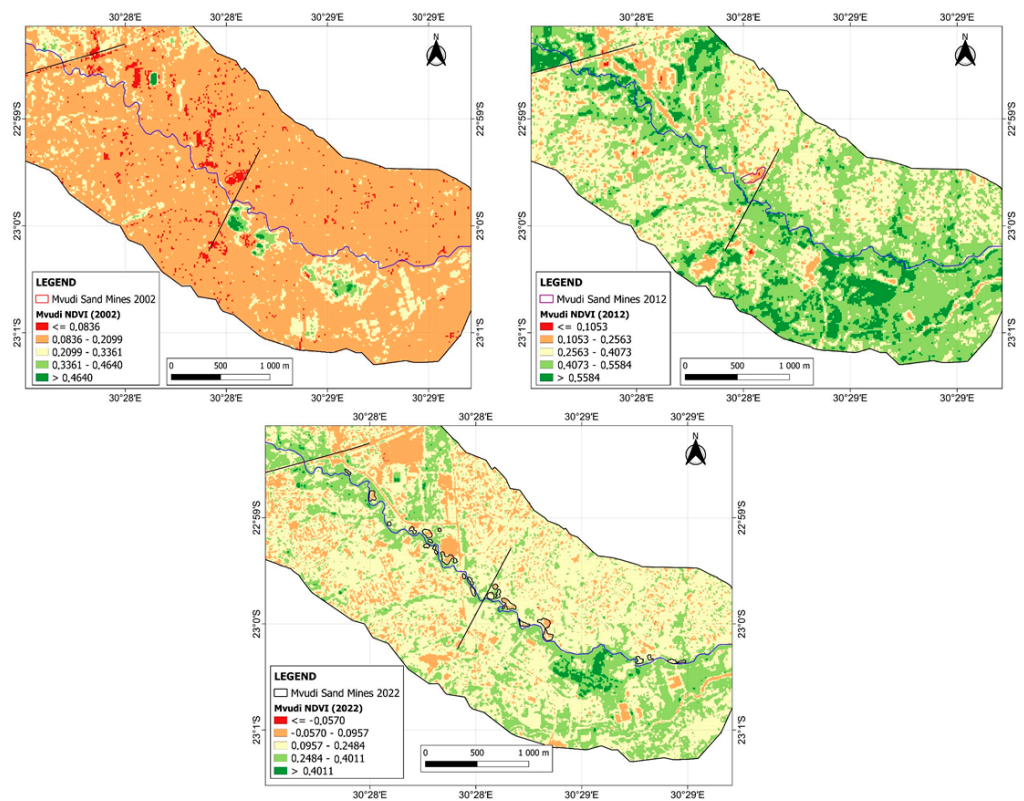


Figure 8. NDVI values of the mining areas and surroundings during periods of active mining.

3.1.2. Sand Mining in the Nzhelele River System

Twenty-seven (27) mining sites were identified along and within the Nzhelele River channel. The mining activities extend over all three river sections (Figure 9a), with the upper stream characterised by more than 50% of them. The town of Makhado is situated within the vicinity of the upper stream. The location of this town might influence the proliferation of illegal mining hotspots in the upper section of this river because there are settlements within this area where new houses and related infrastructures are being built. On the other hand, in the lower sections of the river, the least number of mining locations were found compared to the other two river sections. Such a pattern might be ascribed to the sparsely populated human settlements in the lower sections of the Nzhelele River system, thus suggesting comparatively less exploitation of the available river sands.

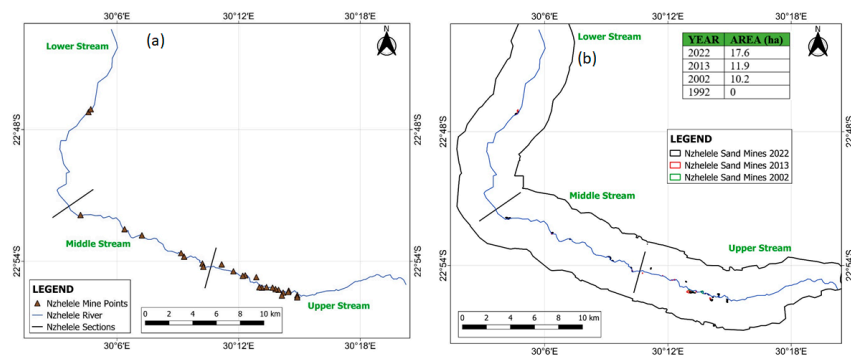


Figure 9. (a) Mining points within and along the Nzhelele River channel. (b) The areal extent of mining activities over the study period in Nzhelele River.

The results revealed that mining activities in the Nzhelele River started after the year 1992. In terms of the areal extent of mining activities over the study period, by the year 2002, mining activities covered an area of 10.2 ha. This value increased by 1.7 ha in 2013.

From the year 2013 to 2022, the areal extent of mining activities increased by 6.7 ha, thus covering a total area of 17.6 ha (Figure 9b).

The LULC maps of the Nzhelele River attained overall accuracies and Kappa coefficients of over 80% and 0.8%, respectively (overall accuracies = 99.30% and Kappa coefficients = 0.99) (Figure 10), which represent reliable mapping. However, the problem of low separability measures of bare land and built-up areas due to spectral similarities is also the case in the LULC maps of the Nzhelele River area since some of the mining locations were classified as built-up zones. Similarly, the same results have been reported in related studies [45], where low separability measures of bare land and built-up areas in such zones were indicative of active mining. The LULC maps for periods of active mining activities are shown in Figure 11. As indicated, in the year 2002, mining activities were restricted to the upper section of this river, and from that time, mining activities spread to other areas in and around this river system. This could be an indication that the sought-after natural resources in the upper sections were gradually being depleted, thus forcing illegal miners to explore exploitable sites along the same river corridor. A similar trend has been reported in a related study [45].

For visibility purposes, the LULC maps are displayed as individual river sections for each period of active mining activities (Figure 11). Some mining locations showed distinct patterns that set them apart from their surroundings. However, in a case where a mining location is surrounded by bare land, it is difficult, if not impossible, to establish a distinct pattern of mining activities. On the contrary, with Google Earth technology, one can detect rugged surfaces and uneven tones, which set mining locations apart from the bare land surfaces that are not related to mining activities.

The NDVI maps representing periods of active mining activities are shown in Figure 12. The NDVI values associated with mining locations were less than 0.2, thus indicating poor vegetation condition and the presence of bare land, which is indicative of mining activities. The NDVI maps were further segmented into individual river sections for visibility purposes (Figure 12).

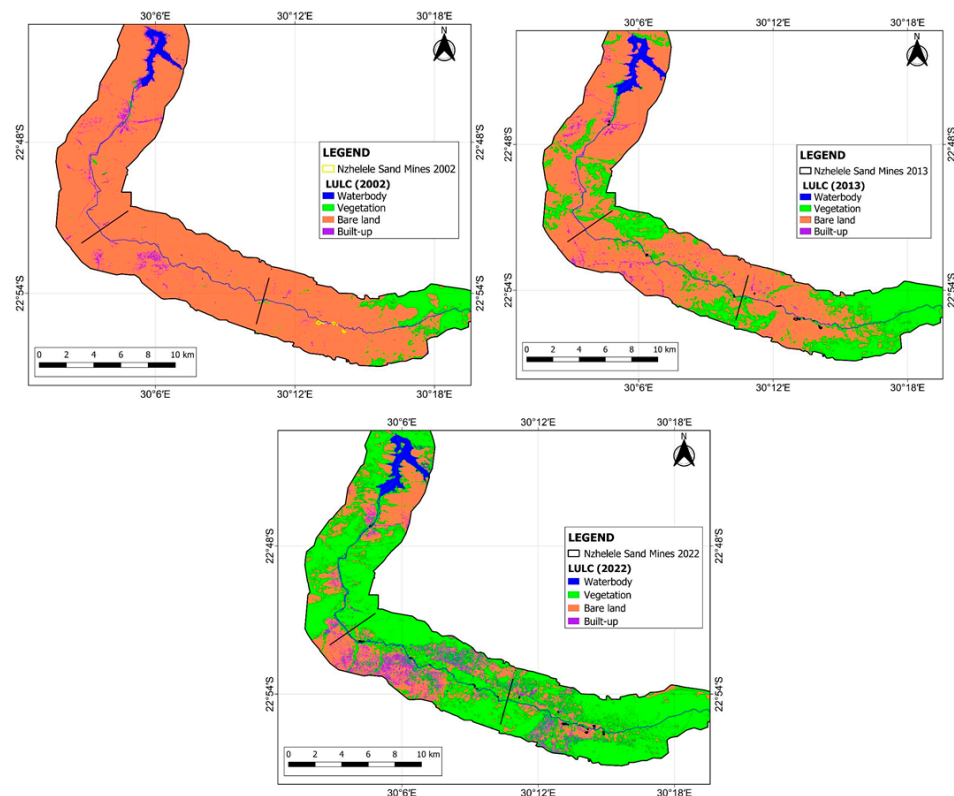


Figure 10. LULC maps of active mining periods in the Nzhelele River channel.

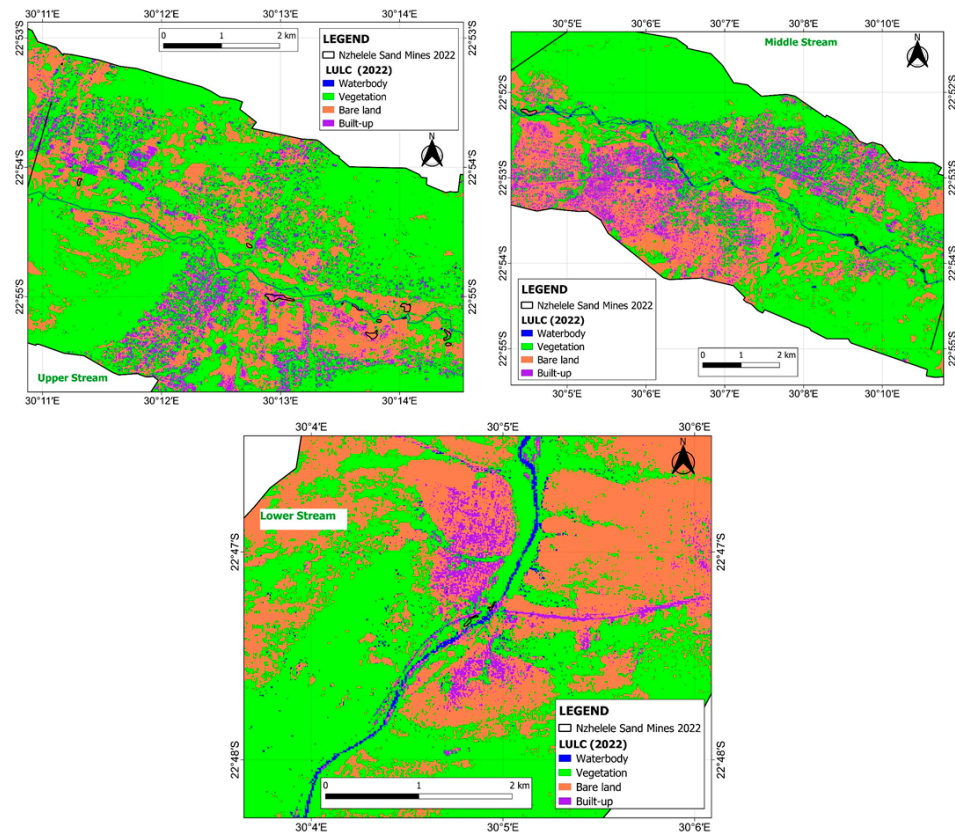


Figure 11. Nzhelele LULC map for the year 2022.

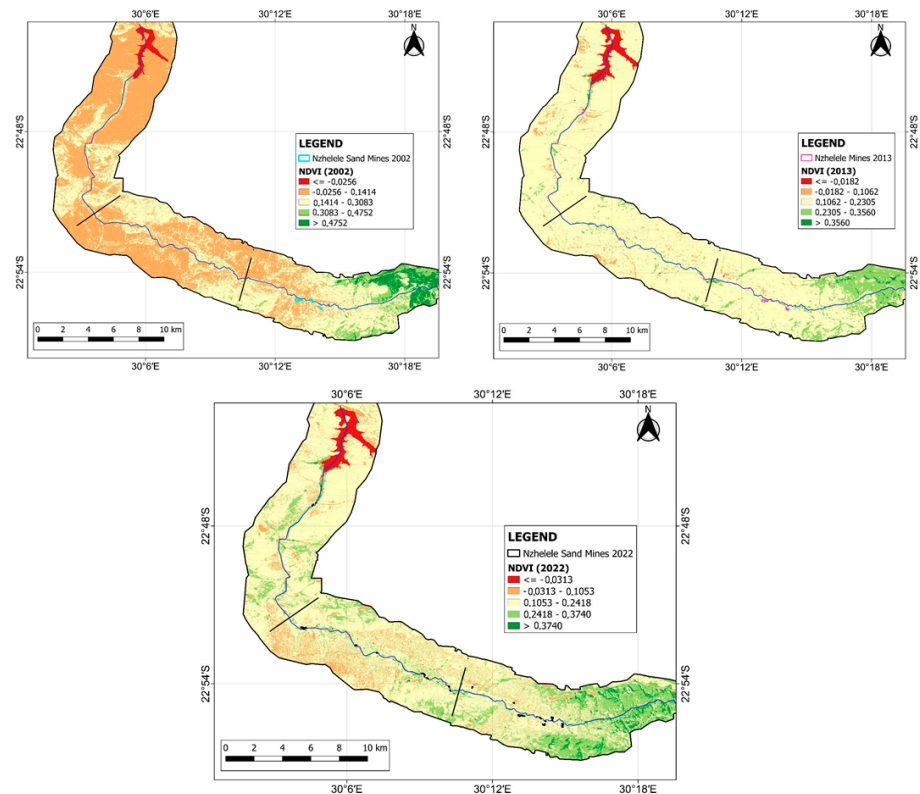


Figure 12. Nzhelele NDVI maps of periods of active mining.

3.1.3. Sand Mining in the Letsitele River System

Seven (7) mining locations were identified along the Letsitele River. The mining activities were limited to the upper and middle stream sections (Figure 13). Among the seven locations, six fell within the middle sections, and one was located in the upper section. Both the middle and upper sections are flanked by human settlements to the north and south directions. However, settlements around the lower streams are found only in the southern sites of this river channel. Furthermore, to the north of the middle sections, which hosted about 85% of mining locations, are industrialised and urbanised areas with relatively well-developed infrastructure in the form of roads, houses, schools, colleges, and recreational facilities. This finding further supports the view that the increased occurrence of sand mining sites is partly accentuated by the development of houses and associated infrastructures in a particular area. Mining activities along this channel started after the year 1992. In terms of the extent of mining activities over the study period, by the year 2002, only an area of 0.32 ha was mined. However, from the year 2002 until 2013, adjoining areas in and around Letsitele River underwent significant mining activities, leading to a total area of 9.65 ha. This increasing trend decreased in the year 2022. At that time, mining activities in the Letsitele River covered only an area of 3.85 ha, which is about a 55% decline in area coverage since the year 2013.

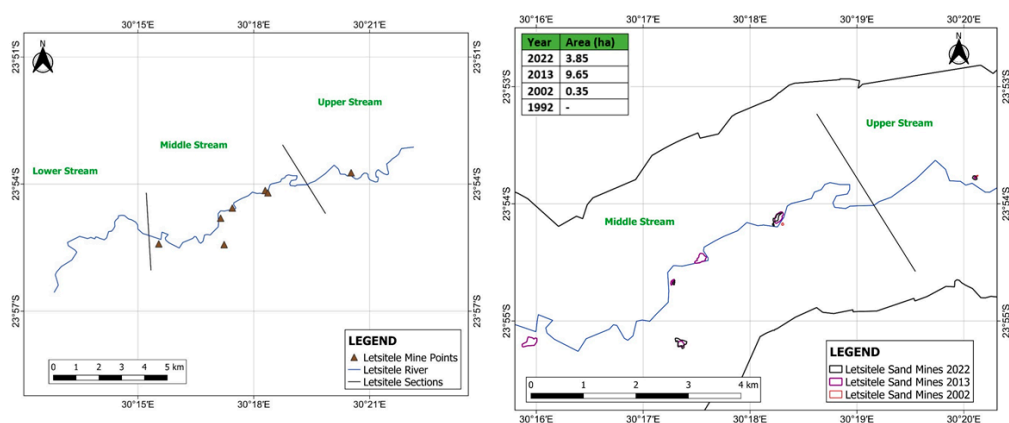


Figure 13. Letsitele river sand mining locations, Area coverage of sand mining activities of the study period.

The LULC maps pertaining to the Letsitele River attained overall accuracies and Kappa coefficients of over 80% and 0.8% (overall accuracies = 93.98% and Kappa coefficients = 0.91), respectively, which represent a reliable LULC mapping. Similarly, the issue of low separability measures of bare land and built-up areas owing to spectral similarities is featured in the LULC maps of Letsitele. The LULC maps for periods of active mining activities are shown in Figure 14. All mining location polygons were classified as bare land except for one location at the western end of the LULC map of the year 2013. Most of these mining locations do not show distinct patterns because their surroundings are predominately characterised by bare land. As stated previously, it is impossible to identify any distinct pattern of mining activities in LULC maps if their surroundings are characterised by bare land.

The NDVI maps that show periods of active mining activities along Letsitele Rive are shown in Figure 15. The NDVI values associated with mining locations were less than 0.2, thus indicating poor vegetation conditions and the presence of bare land, which is a diagnostic feature of mining activities.

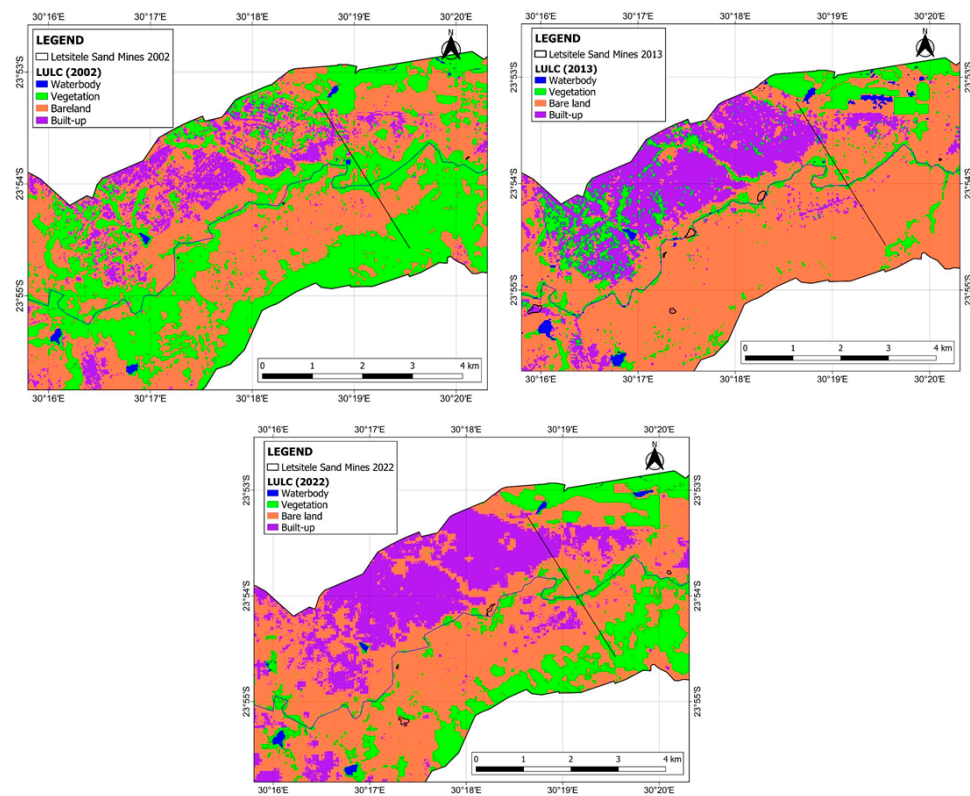


Figure 14. LULC maps of Letsitele River for the periods of active mining activities.

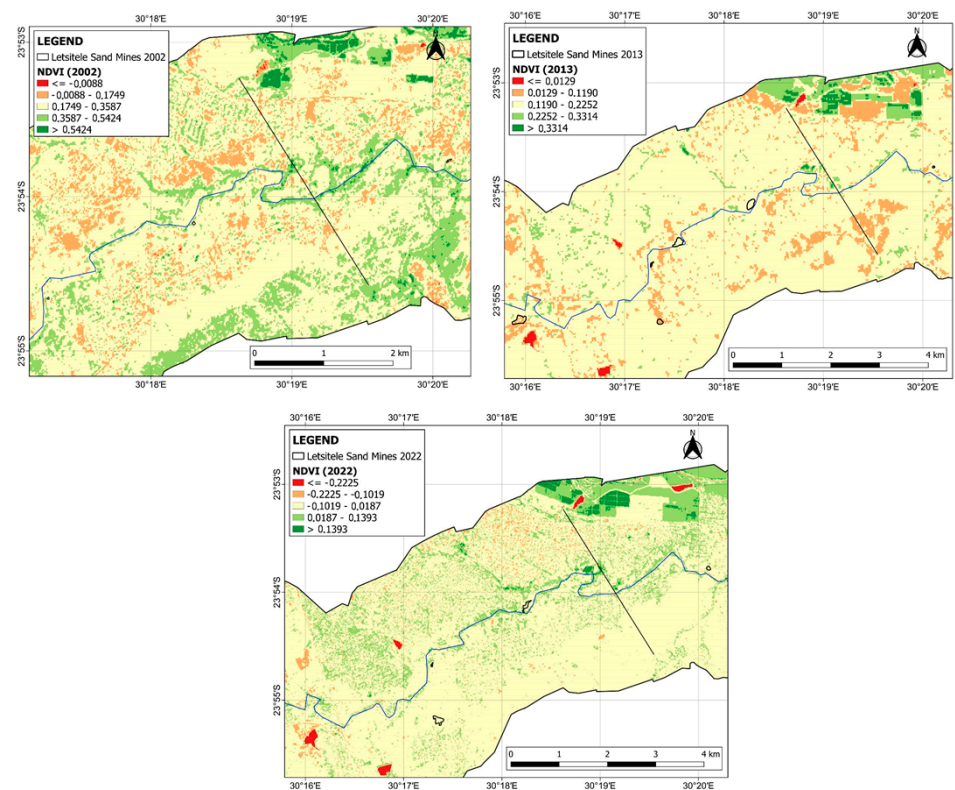


Figure 15. NDVI maps of Letsitele River for the periods of active mining activities.

3.1.4. Sand Mining in the Turfloop River System

A total of 18 sand mining locations were identified along and within the Turfloop River channel. Each river section exhibited six sand mining locations (Figure 16). The areas

adjoining the river channel are mostly comprised of rural areas, and a larger proportion of available land is unoccupied. Mining activities along and within this river channel commenced after the year 2002, and by the year 2013, these activities occupied an area of 9.7 ha. Nevertheless, the areal extent of mining activities increased by a factor of four by the year 2022, with an areal coverage of 43.9 ha (Figure 16).

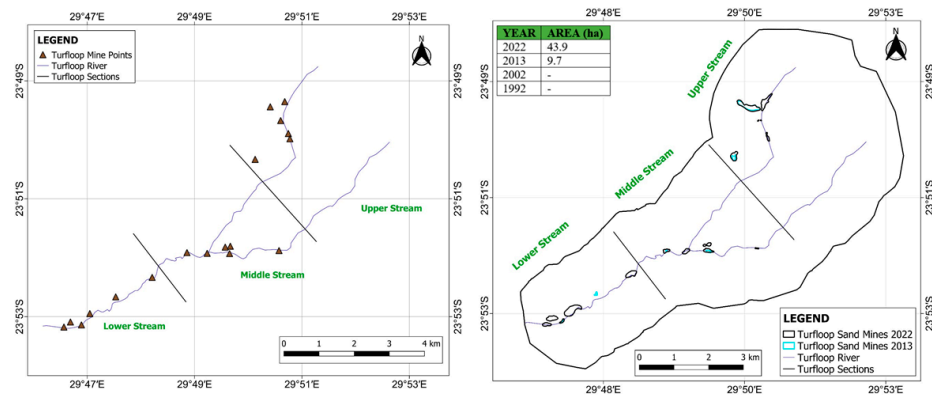


Figure 16. Turfloop River sand mining points, Areal extent of mining areas within and along Turfloop River channel.

The LULC maps of the periods of active mining activities in the Turfloop River are shown in Figure 17. All maps attained overall accuracies and Kappa coefficients beyond 80% and 0.8% (overall accuracies = 99.90% and Kappa coefficients = 0.99), respectively. From the two LULC maps of the periods of active mining from 2013 to 2022, there was a significant increase of built-up areas. The four-fold increase in the areal extent of mining sites may be attributed to the proliferation of such infrastructure developments. As mentioned already, the harvesting of local sand is associated with an increased demand for such materials for building purposes in the same local areas. This is because if such materials are to be transported further away, transport costs may rise, thus making such practices unaffordable.

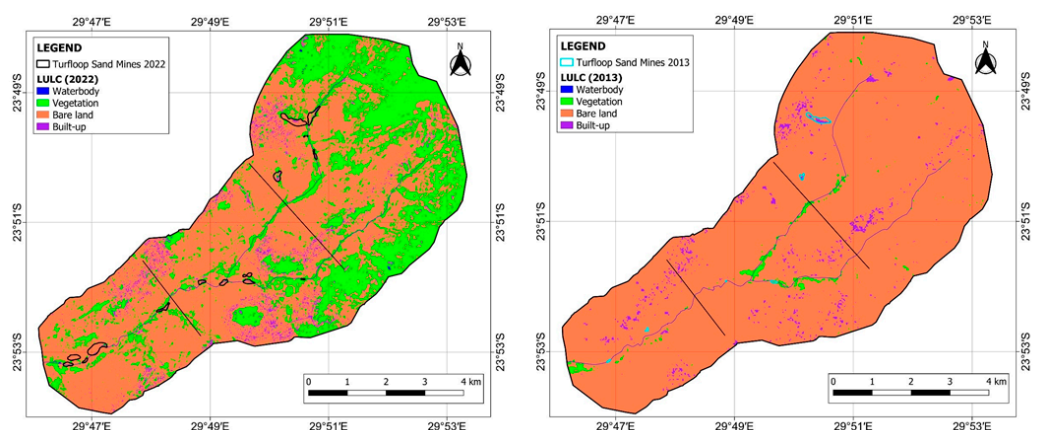


Figure 17. LULC maps of periods of active mining in Turfloop River.

The NDVI maps of periods of active mining activities along the Turfloop River are shown in Figure 18. The NDVI values associated with mining locations were less than 0.2, which suggests poor vegetation conditions and productivity levels and also indicates the presence of bare land, which is diagnostic of mining activities. Another remarkable feature in the NDVI maps is that the majority of the land was characterised by NDVI values of less than 0.2. Though some of this land is classified as vegetation in the LULC maps, particularly the LULC map of the year 2022 (Figure 18), the low NDVI values suggest poor veld conditions and low productivity levels of the existing vegetation in the Turfloop area.

In general, the Turfloop area is situated in an arid region, which adds to the existing poor vegetation conditions.

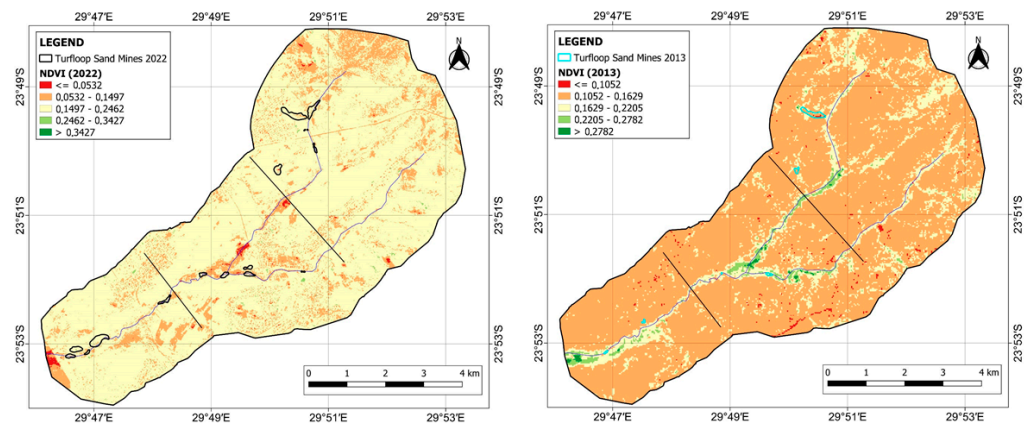


Figure 18. NDVI maps of periods of active mining in Turfloop River.

3.1.5. Sand Mining in the Dwars River System

A total of fourteen (14) sand mining locations were identified along and within the Dwars River channel. The lower, middle, and upper sections are characterised by nine, four, and one mining locations, respectively (Figure 19). Similarly to the Turfloop River system, mining activities along and within the Dwars River channel commenced after the year 2002. By the year 2013, these activities occupied an area of 6.3 ha. The areal extent of mining activities also recorded a fourfold increase by the year 2022, with an area of 23.2 ha. It is important to note that although the upper section of this water corridor is characterised by one mining location, by the year 2022, this location was one of the largest mining areas in terms of areal coverage (Figure 19).

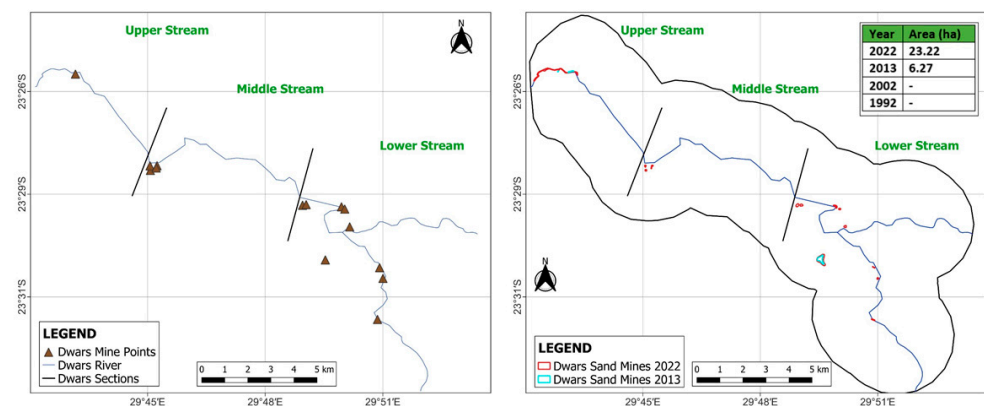


Figure 19. Mining locations along and within Dwars River, areal extent of mining activities in Dwars River.

The LULC maps of the periods of active mining activities in the Dwars River are shown in Figure 20. All maps attained overall accuracies and Kappa coefficients beyond 80% and 0.8 (overall accuracies = 99.90% and Kappa coefficients = 0.99), respectively. It is evident from the two LULC maps of the periods of active mining that the lower and middle sections are characterised by a large number of pixels classified as built-up areas as compared to the upper streams. However, the extensive mining activities taking place at the individual (only one site) mining location in the upper sections may suggest that in the future, infrastructural developments in this section could also increase, given that there is still considerable unoccupied land. This may even prompt further sand exploitation since the sand in this dry river section is well exposed.

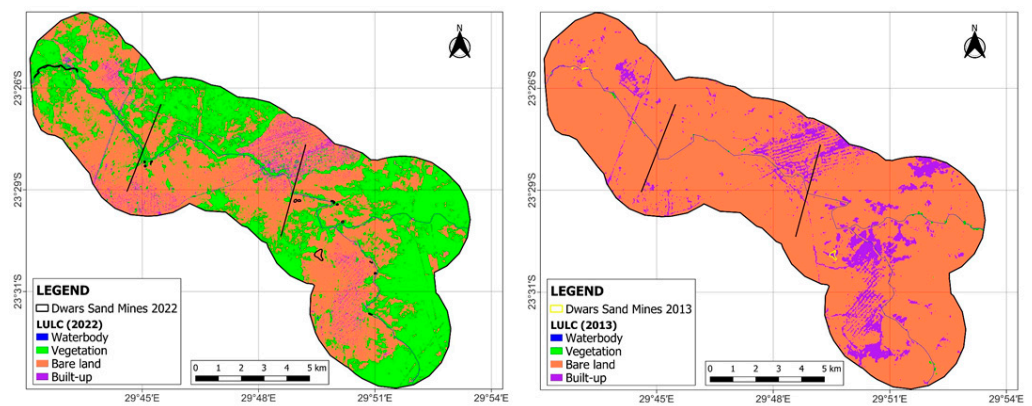


Figure 20. LULC maps of active mining periods in Dwars River.

The NDVI maps of periods of active mining activities along the Dwars River are shown in Figure 21. The NDVI values associated with mining locations were less than 0.2, which suggests poor vegetation conditions and productivity rates and also indicates the presence of bare land, which is indicative of mining activities. Like in the case of Turfloop River, the majority of the land is characterised by NDVI values of less than 0.2. Though some of this land is classified as vegetation in the LULC maps, particularly the LULC map of the year 2022, the low NDVI values suggest poor land conditions and low productivity levels in the existing vegetation. The Dwars and Turfloop River systems are situated about 30 km apart in the arid region and show similarities in terms of the commencement of mining activities and their increasing four-fold trend from the year 2013 to 2022.

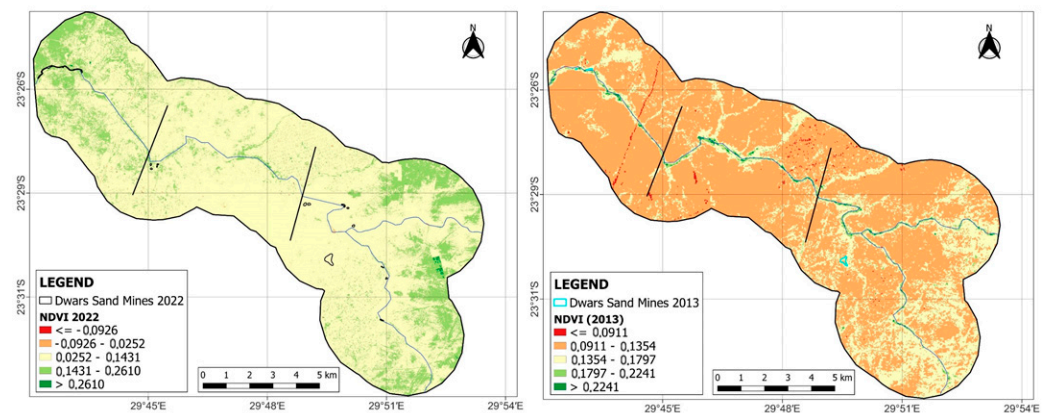


Figure 21. NDVI maps of periods of active mining in Dwars River.

3.1.6. Sand Mining in the Molotosi River System

Three illegal sand mining locations were identified within the Molotosi River channel. The locations are situated within the dry lower stream section (Figure 22). Mining activities in this section commenced after the year 2010. The occurrence of these activities is within the establishment of the Sasamele Brick Yard, which is situated immediately adjacent to the western bank of the river channel. By the year 2013, mining activities covered only an area of 0.4 ha, which increased to almost 4 ha by the year 2022 (Figure 22). This implies that from the year 2013 to 2022, mining activities increased tenfold in the Molotosi River.

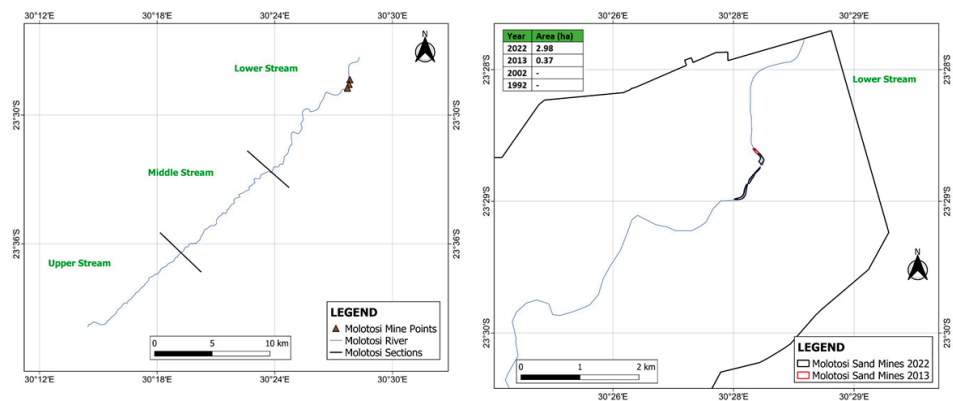


Figure 22. Mining locations in Molotosi River, Areal extent of mining activities in Molotosi River.

The LULC maps of the periods of active mining activities in the Molotosi River are shown in Figure 23. All maps attained overall accuracies and Kappa coefficients beyond 80% and 0.8 (overall accuracies = 92% and Kappa coefficients = 0.90), respectively. The issue of low separability measures of bare land and built-up areas owing to spectral similarities is also the case even in the LULC maps of the Molotosi River. All three mining locations are classified as built-up areas.

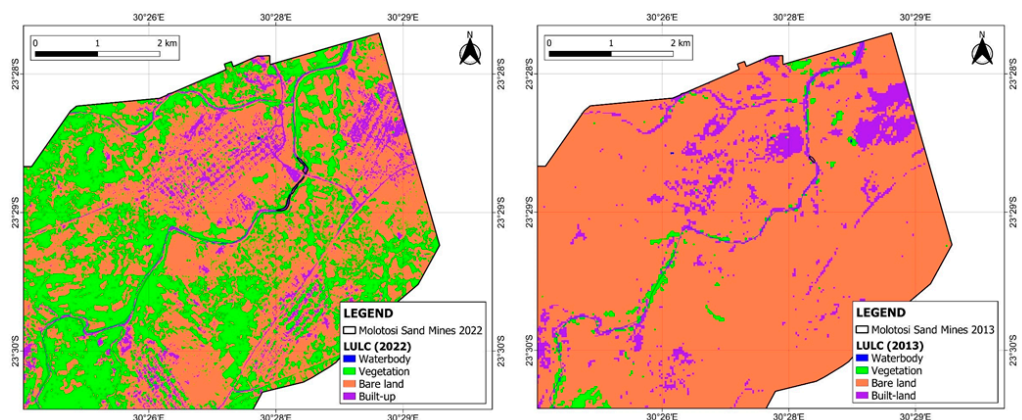


Figure 23. LULC maps of active mining periods in Molotosi River.

On the other hand, the NDVI maps of periods of active mining activities within Molotosi River are shown in Figure 24. The NDVI values associated with mining locations were less than 0.2, thus indicating poor vegetation conditions and productivity. The presence of bare land is a diagnostic feature of mining activities.

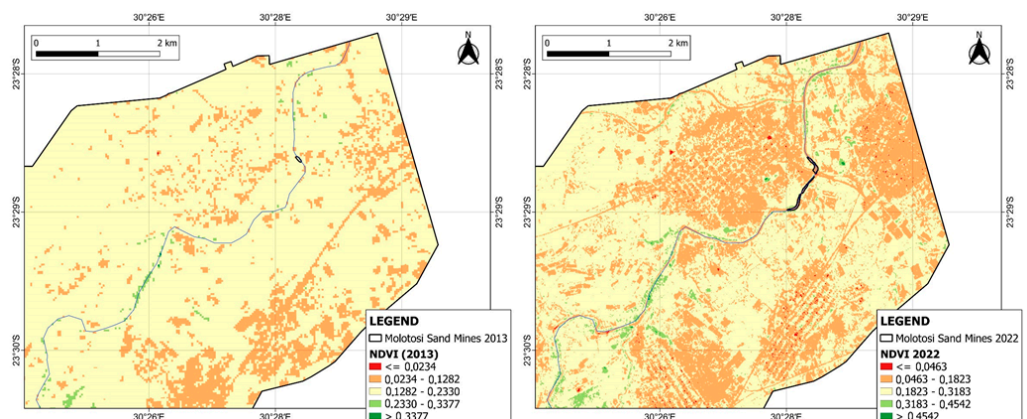


Figure 24. NDVI maps of active mining periods in Molotosi River.

3.1.7. Sand Mining in the Mokolo River System

A total of six (6) illegal sand mining locations were identified along and within the Mokolo River channel. The mining locations are limited to the upper section of this river (Figure 25). The upper section is the only section along the Mokolo River with infrastructural developments. As stated previously, sand mining is driven by the demand for material inputs needed in the construction of houses and associated infrastructure. Mining in this section started after the year 2002, and by the year 2013, mining activities covered an area of about 31.5 ha. By the year 2022, the areal extent of these activities decreased by 8.6 ha, covering an area of 22.8 ha (Figure 25).

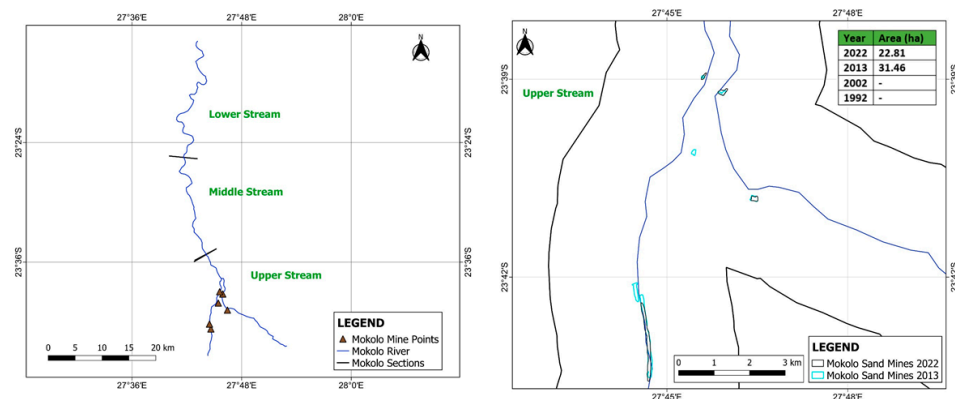


Figure 25. Mining locations of Mokolo River, Areal extent of mining activities in Mokolo River.

The LULC maps of the periods of active mining activities in the Mokolo River are shown in Figure 26. All maps attained overall accuracies and Kappa coefficients beyond 80% and 0.8% (overall accuracies = 98.21% and Kappa coefficients = 0.97), respectively. The issue of low separability measures of bare land and built-up areas owing to spectral similarities is also the case even in the LULC maps of the Mokolo River. Some parts within mining polygons were classified as built-up zones. Nonetheless, most mining locations showed distinct patterns that set them apart from their surroundings, which are mostly characterised by vegetation cover (Figure 26).

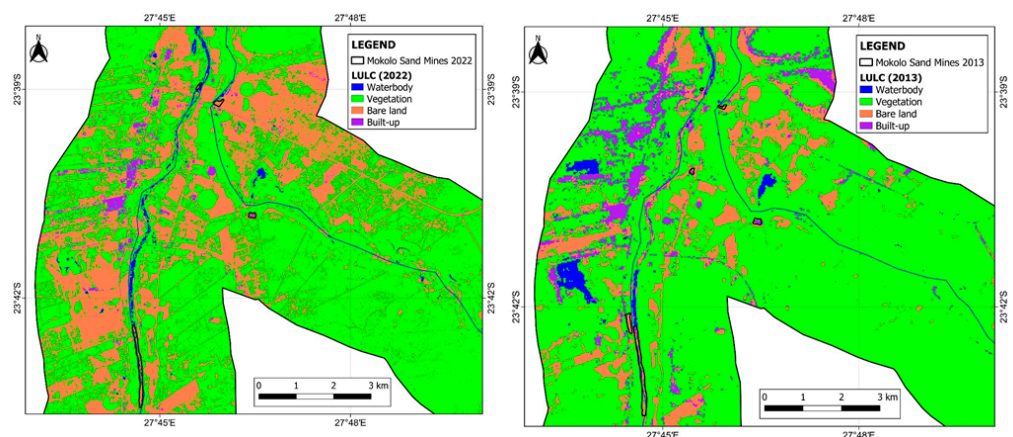


Figure 26. LULC maps of periods of active mining activities.

NDVI maps indicating periods of active mining activities within the Mokolo River are shown in Figure 27. The NDVI values associated with mining locations were less than 0.2, indicating poor vegetation conditions and productivity rates. The areas shown have bare land, which is a diagnostic feature of mining activities.

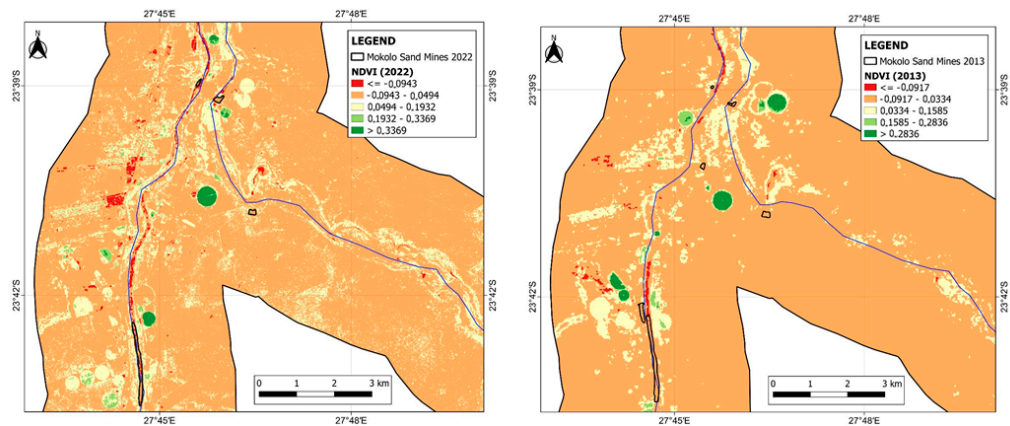


Figure 27. NDVI maps of active mining periods in Mokolo River.

3.2. Prediction of the Future Extent of River Sand Mining Activities

A regression analysis was conducted to develop predictive models that can shed light on the future extent of illegal sand mining activities in the study area. The models exhibited varying degrees of accuracy based on their R-squared values. The results of the study have shown that the predictive models in all large rivers had R-squared values less than 80%, which is not recommended in this study. A closer examination of the causes of such results was taken into consideration. For example, rivers such as Mokolo and Letsitele exhibited an R-squared value of 66% and 51%, respectively (Figure 28).

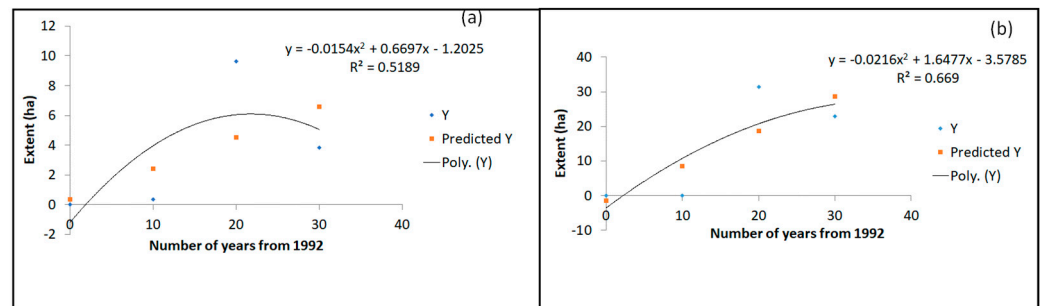


Figure 28. (a) Predictive model for the Letsitele River (b) predictive model for Mokolo River.

These are some of the largest rivers or catchments (with a width greater than 100 m) and above found in the province. It is expected that during heavy rainfall, some of the previous illegal sand mining pits will be filled with sediments (sand). Therefore, the extent of such rivers is difficult to predict. Owing to the previous findings, better predictions were also made in some of the catchments (with less than 100 m width), which were not considered to be large rivers, and the predictions ranged from 92% to 99% (Figure 29).

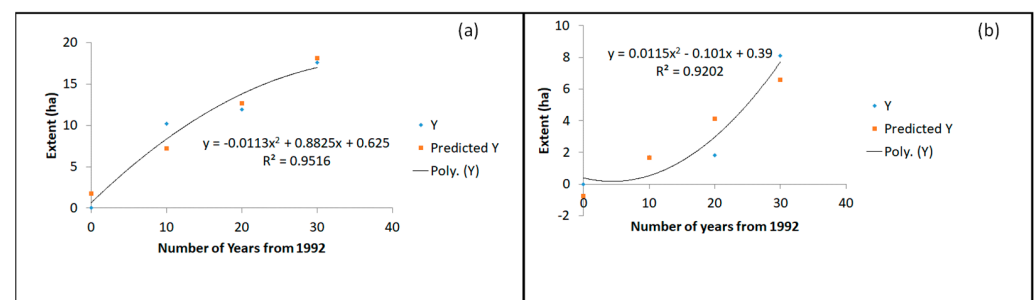


Figure 29. (a) Predictive model for the Nzhelele River, (b) predictive model for the Mvudi River.

As depicted in Figure 29a,b, in terms of the extent of river sand mining in the coming 40 years from the year 1992, it was predicted that the Turfloop River catchment (see Figure 30a,b) is expected to have an area of approximately 92.415 ha affected by illegal river sand mining. In the environs of the Dwars river system (Figure 31), the extent of sand mining activities will increase to 48 ha (Figure 31a).

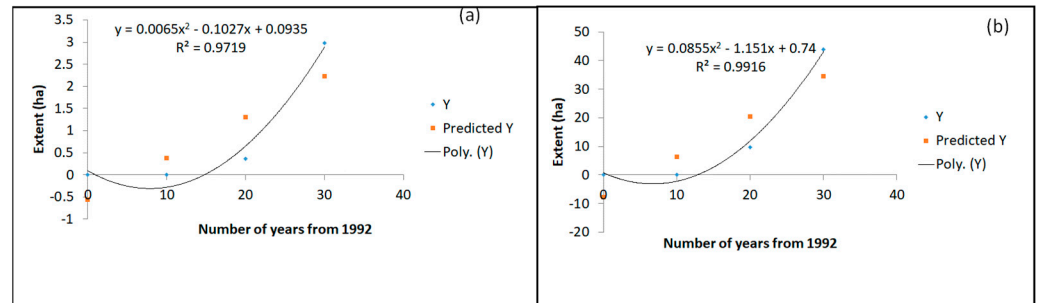


Figure 30. (a) A predictive model for the Molototsi River. (b) A predictive model for Turfloop River.

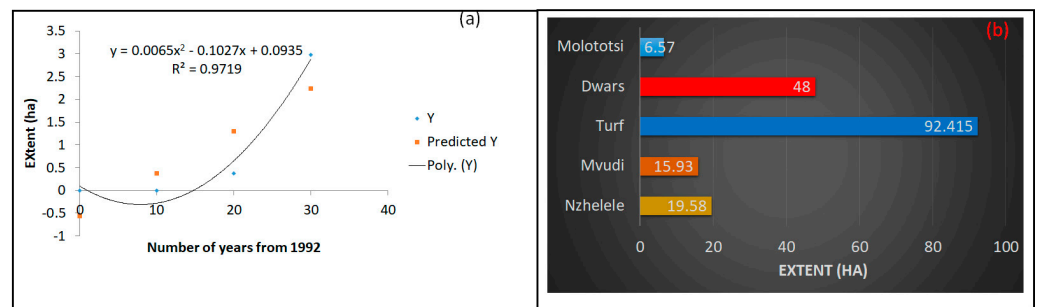


Figure 31. (a) A predictive model for the Dwars River. (b) Estimated extent of river sand mining in 40 years' time from 1992.

By contrast, in the other catchments, future predictions yielded lower values in the size of lands to be affected by illegal river sand mining activities. More specifically, the models revealed that in the areas adjoining the Nzhelele and Mvudi river systems, areas to be impacted by illegal sand mining would amount to 19.58 ha and 16.93 ha, respectively (Figure 31b). Lastly, the area susceptible to future river sand mining in the next 10 years was only 6.57 ha in the Molototsi River catchment (Figure 31b).

4. Conclusions

The study aimed to assess the extent of river sand mining activities across some of the catchments in Limpopo Province, South Africa. This was followed by the determination when sand mining activities commenced in each of the individual catchments. Thus, remote sensing was applied to predict the extent of river sand mining from the year 1992 to 2022, and statistical prediction models were utilised to predict the extent of sand mining for the next 10 years.

Based on all of the analysed data in this study, sand mining activities started from the year 1992 to 2022. Such activities were identified through the detection of image elements, such as shape, tone, size, association, pattern, and others, by means of Google Earth technology. The mining areas were easily identifiable, given their irregular shape and sizes, rugged surfaces and uneven tones, which set them apart from their surroundings. For the most part, mining locations appeared as bare land surfaces in the LULC classification map and were characterised by low NDVI values (<0.2). Such low values are associated with low vegetation productivity and poor vegetation conditions in the catchments under consideration.

The results of the study have shown that most of the catchments started to experience illegal sand mining activities from the year 1992, though the extraction was relatively low.

Equally, a decrease in vegetation coverage across the river systems has been indicated, which also suggests that the extraction of sand and gravel has increased. Following that, a close look at the extent of river sand mining has shown that Turfloop River may experience a large extraction ratio in the coming 10 years, with about 92.415 ha of land expected to be affected. It was also indicated that the Molototsi River, which has been the least affected system with a reduced extraction ratio of about 6.57 ha, is expected to suffer increased exploitation in the next 10 years' time. The predictive models were also developed across all these rivers, and the most accurate model was within the Turfloop River system, followed by the Dwars and Molototsi Rivers, as supported by some of the previous studies documented in this paper.

In terms of scientific contribution, it has been evident from the results of this study and other previous studies globally that the ever-increasing demand for sand for construction and infrastructural developments results in the increase of river sand mining activities, as well as the associated environmental impacts, such as habitat degradation, deforestation, and altered river systems and functionalities. Indeed, the results of this study correlate very well with similar studies performed in other countries by finding that the amount of sand being extracted is increasing at a faster rate than it can be replaced, and as a result, channel floodplains and deltas are suffering from a severe lack of sand. Because of this, the current study further develops simple predictive models on the future extractions of sand, provided the situation remains similar. Owing to that, the predictive models correlate very well with the observations made throughout the years, and it is expected that sand resources will be much more depleted if no action has been taken. It is therefore recommended that efforts should be focused on the regulation of sand extraction and the promotion of environmental impact assessments (EIAs) by the relevant authorities, including government departments and local municipalities so that permits, licenses, and tariffs can be issued for sand mining. This will help to mitigate the effects of land degradation, which are a direct result of sand mining. Another important scientific contribution of this study was to demonstrate how digital image processing and remote sensing methods may be used as a tool for monitoring the extent of illegal river sand mining in a possible affected area. Therefore, if the method is highly considered and adopted, this will allow the regulatory agencies responsible for monitoring illegal sand mining to do so in a more efficient manner and will help avoid or minimise the adverse effects of illegal mining.

Author Contributions: Conceptualization, M.T.D.R., I.T.R. and F.S.; methodology, M.T.D.R., I.T.R. and F.S.; software, M.T.D.R., I.T.R. and F.S.; validation, M.T.D.R., I.T.R. and F.S.; formal analysis, M.T.D.R., investigation, M.T.D.R.; resources, M.T.D.R., I.T.R. and F.S.; data curation, M.T.D.R.; writing—original draft preparation, M.T.D.R.; writing—review and editing, I.T.R. and F.S.; visualisation, M.T.D.R.; supervision, I.T.R. and F.S.; project administration, I.T.R. and F.S.; funding acquisition, M.T.D.R. All authors have read and agreed to the published version of the manuscript.

Funding: The APC was funded by Professor Rampedi, I.T. (MDPI reviewing vouchers) and University of Limpopo, Department of Geology and Mining (Departmental research funds).

Data Availability Statement: All data generated or analysed during this study are included in the paper.

Acknowledgments: The authors wish to thank the University of Johannesburg and the University of Limpopo for providing funding.

Conflicts of Interest: The authors declare no conflict of interest.

References

1. Duan, H.; Cao, Z.; Shen, M.; Liu, D.; Xiao, Q. Detection of illicit sand mining and the associated environmental effects in China's fourth largest freshwater lake using daytime and nighttime satellite images. *Sci. Total Environ.* **2019**, *647*, 606–618. [[CrossRef](#)] [[PubMed](#)]
2. Lai, X.; Huang, Q.; Zhang, Y.; Jiang, J. Impact of lake inflow and the Yangtze River flow alterations on water levels in Poyang Lake, China. *Lake Reserv. Manag.* **2014**, *30*, 321–330. [[CrossRef](#)]

3. Meng, X.; Jiang, X.; Li, Z.; Wang, J.; Cooper, K.M.; Xie, Z. Responses of macroinvertebrates and local environment to short-term commercial sand dredging practices in a flood-plain lake. *Sci. Total Environ.* **2018**, *631–632*, 1350–1359. [[CrossRef](#)]
4. Zeng, X.; Xu, L.; Liu, J.; Wu, Y.; Yu, Z. Occurrence and distribution of organophosphorus flame retardants/plasticizers and synthetic musks in sediments from source water in the Pearl River Delta, China. *Environ. Toxicol. Chem.* **2018**, *37*, 975–982. [[CrossRef](#)]
5. Zhao, M.; Dewei, Y.; Ping, W.; Ping, S. A marketbased approach to marine sand resource management in the Pearl River estuary, China. *Ocean Coast. Manag.* **2015**, *105*, 5664.
6. Chilikova-Lubomirova, M. River systems under the anthropogenic and climate change impacts: Bulgarian case. In *Water Resources Management in Balkan Countries*; Negm, A., Romanescu, G., Zelenakova, M., Eds.; Springer: Cham, Switzerland, 2020; pp. 327–355.
7. Filho, W.L.; Hunt, J.; Lingos, A.; Platje, J.; Vieira, L.W.; Will, M.; Gavrilitea, M.D. The Unsustainable Use of Sand: Reporting on a Global Problem. *Sustainability* **2021**, *13*, 3356. [[CrossRef](#)]
8. Rahman, M.A.; Zaman, M.N.; Biswas, P.K.; Sultana, M.S. Economic Viability of the Tista River Sand Deposits in Bangladesh an Overview. *J. Sci. Res.* **2017**, *9*, 219–233. [[CrossRef](#)]
9. Pitchaiah, P.S. Impacts of Sand Mining on Environment—A Review. *SSRG Int. J. Geo Inform. Geol. Sci.* **2017**, *4*, 1–5.
10. Indian Bureau of Mines. *Government of India Ministry of Mines Indian Bureau of Mines*; Indian Bureau of Mines: Nagpur, India, 2016.
11. Gathogo, M.P.; Amimo, M.O. Social Environmental Effects of River Sand Mining: Case Study of Ephemeral River Kivou in Kitui County, Kenya. *IQSR J. Humanit. Soc. Sci.* **2017**, *22*, 3137.
12. Gitonga, E.K. Factors Affecting Sand Harvesting in Machakos County. Master’s Thesis, University of Nairobi, Nairobi, Kenya, 2013.
13. Akanwa, A.O. River Sand Mining and Its Ecological Footprint at Odor River, Nigeria. In *Agroecological Footprints Management for Sustainable Food System*; Banerjee, A., Meena, R.S., Jhariya, M.K., Yadav, D.K., Eds.; Springer: Singapore, 2021.
14. Atejoye, A.A.; Odeyemi, C.A. Analysing impact of sand mining in Ekiti State, Nigeria using GIS for sustainable development. *World J. Res. Rev.* **2018**, *6*, 262696.
15. Maeko, M.P. An Evaluation of the Ecological Impacts of Sand Mining on the Mokolo River in Lephalale, South Africa. Doctoral Dissertation, University of South Africa, Pretoria, South Africa, 2020.
16. Sengani, F.; Zvarivadza, T. The Impact of Sand Mining on the Fluvial Environment: Case Study of Nzhelele River in Limpopo Province, South Africa. In *Proceedings of the 18th Symposium on Environmental Issues and Waste Management in Energy and Mineral Production*; WidzykCapehart, E., Hekmat, A., Singhal, R., Eds.; SWEMP 2018; Springer: Cham, Switzerland, 2019.
17. Gondo, T.; Mathada, H.; Amponsah-Dacosta, F. Regulatory and policy implications of sand mining along shallow waters of Njelele River in South Africa. *Jambá J. Disaster Risk Stud.* **2019**, *11*, 727. [[CrossRef](#)] [[PubMed](#)]
18. Mngeni, A.; Musampa, C.M.; Nakin, M.D.V. The effects of sand mining on rural communities. *WIT Trans. Ecol. Environ.* **2017**, *210*, 443–453. [[CrossRef](#)]
19. Chevallier, R. Illegal Sand Mining in South Africa. *Gov. Afr. Resour. Programme Policy Briefing* **2014**, 116.
20. Kori, E.; Mathada, H. An assessment of environmental impacts of sand and gravel mining in Nzhelele Valley, Limpopo Province, South Africa. In *3rd International Conference on Biology, Environment and Chemistry*; IACSIT Press: Singapore, 2012; Volume 46, p. 137141.
21. Madyise, T. Case Studies of Environmental Impacts of Sand Mining and Gravel Extraction for Urban Development in Gaborone. Doctoral Dissertation, University of South Africa, Pretoria, South Africa, 2013.
22. Debrah, A.A.; Watson, I.; Quansah, D.P.O. Comparison between artisanal and smallscale mining in Ghana and South Africa: Lessons learnt and ways forward. *J. S. Afr. Inst. Min. Metall.* **2014**, *114*, 913921.
23. Muiruri, P.G.; Obando, J.A.; Mahiri, I.O. Active morphological factors determining the locations of sand mines in dry-river channels. *Eur. J. Sustain. Dev. Res.* **2023**, *7*, em0216. [[CrossRef](#)]
24. Zvarivadza, T. Artisanal and Small-Scale Mining as a challenge and possible contributor to Sustainable Development. *Resour. Policy* **2018**, *56*, 49–58. [[CrossRef](#)]
25. Rupprecht, S. Bench mining utilizing manual labour and mechanized equipment—A proposed mining method for artisanal small-scale mining in Central Africa. *J. S. Afr. Inst. Min. Met.* **2017**, *117*, 25–31. [[CrossRef](#)]
26. Amposahdacosta, F.; Mathada, H. Study of sand mining and related environmental problems along the Nzhelele River in Limpopo Province of South Africa. *Mine Water Circ. Econ.* **2017**, *2*, 12631270.
27. Cai, X.; Magidi, J.; Nhamo, L.; Van Koppen, B. Mapping irrigated areas in the Limpopo Province, South Africa. In *Mapping Irrigated Areas in the Limpopo Province, South Africa*; International Water Management Institute (IWMI): Colombo, Sri Lanka, 2016; Volume 172. [[CrossRef](#)]
28. Ashton, P.J.; Love, D.; Mahachi, H.; Dirks, P.H.G.M. An overview of the impact of mining and mineral processing operations on water resources and water quality in the Zambezi, Limpopo and Olifants Catchments in Southern Africa. In *Contract Report to the Mining, Minerals and Sustainable Development (Southern Africa) Project*; by CSIR-Environmentek, Pretoria and Geology Department, University of Zimbabwe-Harare. Report No. ENV-PC; Mining, Minerals and Sustainable Development: Cape Town, South Africa, 2001; Volume 42, p. 1362.
29. Research Systems Inc. *ENVI Tutorials*; Research Systems Inc.: Boulder, CO, USA, 2008; 18p.
30. Green, A.A.; Craig, M.D. Analysis of aircraft spectrometer data, with logarithmic residuals. In *Proceedings of the Airborne Imaging Spectrometer Data Analysis Workshop*, Sydney, Australia, 8–10 April 1985; p. 111119.

31. Muavhi, N. Evaluation of effectiveness of supervised classification algorithms in land cover classification using ASTER images—A case study from the Mankweng (Turfloop) Area and its environs, Limpopo Province, South Africa. *S. Afr. J. Geomat.* **2020**, *9*, 61–74. [[CrossRef](#)]
32. Muavhi, N. A simple approach for monitoring vegetation change using time series remote sensing analysis: A case study from the Thathe Vondo Area in Limpopo Province, South Africa. *S. Afr. J. Sci.* **2021**, *117*, 1–9. [[CrossRef](#)]
33. Powell, R.L.; Matzke, N.; de Souza, C., Jr.; Clark, M.; Numata, I.; Hess, L.L.; Roberts, D.A. Sources of error in accuracy assessment of thematic land-cover maps in the Brazilian Amazon. *Remote Sens. Environ.* **2004**, *90*, 221–234. [[CrossRef](#)]
34. Daboor, M.; Howell, S.; Shokr, M.; Yackel, J. The Jeffries–Matusita distance for the case of complex Wishart distribution as a separability criterion for fully polarimetric SAR data. *Int. J. Remote Sens.* **2014**, *35*, 6859–6873. [[CrossRef](#)]
35. Swain, P.H.; Davis, S.M. *Remote Sensing: The Quantitative Approach*; McGrawHill Publishers: New York, NY, USA, 1978.
36. Richards, J.A.; Jia, X. *Remote Sensing Digital Image Analysis*, 4th ed.; Springer: Berlin/Heidelberg, Germany, 2006.
37. Latty, R.S.; Hoffer, R.M. Waveband evaluation of proposed Thematic Mapper in forest cover classification. In Proceedings of the Fall Technical Meeting, ACSMASP, Niagara Falls, NY, USA, 1 January 1981.
38. Padma, S.; Sanjeevi, S. Jeffries Matusita based mixed-measure for improved spectral matching in hyperspectral image analysis. *Int. J. Appl. Earth Obs. Geoinf.* **2014**, *32*, 138–151. [[CrossRef](#)]
39. Yu, W.; Liu, T.; Valdez, R.; Gwinn, M.; Khoury, M.J. Application of support vector machine modeling for prediction of common diseases: The case of diabetes and pre-diabetes. *BMC Med. Inform. Decis. Mak.* **2010**, *10*, 16. [[CrossRef](#)] [[PubMed](#)]
40. Dakalira, Y.S.; Mangulama, J.A.; Khemthong, B.; Mudimu, G.T.; Jin, L.; Zuo, T.; Wu, J. Impacts of Artisanal SmallScale Mining in Rural Households: A Case of Mzimba District, Malawi. *J. Poverty Investig. Dev.* **2017**, *37*, 110.
41. Hua, L.; Wang, H.; Sui, H.; Wardlow, B.; Hayes, M.J.; Wang, J. Mapping the spatiotemporal dynamics of vegetation response lag to drought in semiarid region. *Remote Sens.* **2019**, *11*, 1873. [[CrossRef](#)]
42. Nafaji, Z.; Fatchi, P.; Darvishsefat, A.A. Vegetation dynamics trend using satellite time series imagery. *Int. Arch. Photogramm. Remote Sens. Spat. Inf. Sci.* **2019**, *42*, 783–788.
43. Nabegu, A.B. Morphologic Response of a Stream Channel to Extensive Sand Mining. *Res. J. Environ. Earth Sci.* **2014**, *6*, 96–101. [[CrossRef](#)]
44. Pankaj, R. *Riverbank Erosion: A Concise and Critical Review of Scales, Approaches, Methods and Techniques*; Mahi Publication: Dholera, India, 2021.
45. Diaconu, D.C.; Koutalakis, P.D.; Gkiatas, G.T.; Dascalu, G.V.; Zaimes, G.N. River Sand and Gravel Mining Monitoring Using Remote Sensing and UAVs. *Sustainability* **2023**, *15*, 1944. [[CrossRef](#)]

Disclaimer/Publisher’s Note: The statements, opinions and data contained in all publications are solely those of the individual author(s) and contributor(s) and not of MDPI and/or the editor(s). MDPI and/or the editor(s) disclaim responsibility for any injury to people or property resulting from any ideas, methods, instructions or products referred to in the content.